EUROPEAN ORGANIZATION FOR NUCLEAR RESEARCH

CERN-EP/81-86
4 August 1981

THE "LEADING" PARTICLE EFFECT IN HADRON PHYSICS

M. Basile, G. Cara Romeo, L. Cifarelli, A. Contin, G. D'Ali,
P. Di Cesare, B. Esposito, P. Giusti, T. Massam, R. Nania, F. Palmonari, V. Rossi,
G. Sartorelli, M. Spinetti, G. Susinno, G. Valenti, L. Votano and A. Zichichi

CERN, Geneva, Switzerland.
Istituto di Fisica dell'Università di Bologna, Italy.
Istituto Nazionale di Fisica Nuclear, Laboratori Nazionali di Frascati, Italy.
Istituto Nazionale di Fisica Nucleare, Sezione di Bologna, Italy.
Istituto di Fisica dell'Università di Perugia, Italy.
Istituto di Fisica dell'Università di Roma, Italy.

ABSTRACT

A world review is presented of the "leading" particle effect in hadron physics: baryon-baryon, baryon-antibaryon, meson-baryon, and photon-baryon processes are studied and compared with hadron production from an initial state which does not contain any hadron. In this latter case the "leading" effect is not present.

It is shown that the "leading" particle effect is fully present even in hadron interactions initiated by neutrinos.

The importance of the "leading" effect in hadron physics is discussed.

(Submitted to Nuovo Cimento)

1. INTRODUCTION

We have recently introduced a new method for studying hadronic reactions[1]. This method is based on the determination of the effective energy available for particle production. This allows firstly a comparison of the properties of multiparticle final states produced in purely hadronic interactions at different nominal c.m. energies. For example, in a proton-proton interaction at 62 GeV c.m. energy, the two protons can carry 40 GeV of the available energy. In this case the multiparticle system produced should be labelled by an effective energy of 22 GeV, and all quantities such as fractional momentum distribution, average charged multiplicity, transverse momentum distribution, etc., should be labelled with 22 GeV, not 62 GeV. Moreover, in another proton-proton interaction at 52 GeV c.m. energy, the two protons can carry 30 GeV of the available energy. In this case, again the multiparticle system produced should be labelled by the effective energy of 22 GeV. Thus two primary (pp) interactions, at $\sqrt{s}$ = 62 and $\sqrt{s}$ = 52 GeV, can produce identical final states, where the effective energy is 22 GeV. The key point is to subtract the energy taken away by the "leading" particles.

Another important consequence of our method is the extension of the comparison to hadronic final states which are not produced by the same hadrons. For example, (pp) interactions can be compared with (πp), (Kp), and (np) processes. Moreover the comparison can be extended further: even to photon-induced and charged leptons plus neutrino-induced processes: (γp), ($e^{\pm}$p), ($\mu^{\pm}$p), (νp), etc. Finally, the comparison can obviously be extended to final states produced in (e^+e^-) annihilation. The basic point is to take into account the effect of the "leading" hadron which, from the initial to the final state, keeps a highly privileged energy and momentum sharing. This "leading" four-momentum has to be correctly subtracted from the multiparticle final state produced.

This method has been applied extensively[1-9] in the study of multiparticle hadronic systems produced in low-p_T, high-energy, (pp) interactions. The "leading" particle effect has also been applied to identify the presence of a high-energy proton, in order to search for new baryonic states[10-14] in (pp) interactions. In this study, without the "leading" particle effect, it would be impossible to identify the high-energy proton.

The roots of this new approach to the study of hadronic interactions go back a long time, to a proposal by the CERN-Bologna Group to study "leptonic-like" (pp) collisions (CERN/PHI/COM-69/35, 8 July 1969).

The lesson that has been learnt is that, in a given hadronic reaction, it is in fact necessary to disentangle two phenomena,

i) the "leading" particle effect, and

ii) the multihadron production mechanism,

in order to understand the intrinsic features of both effects.

In this paper we present a review of the "leading" particle phenomenon.

In Section 2 we give a definition of the "leading" particle and of the variables used; in Section 3 we show that in $e^+e^- \to$ hadrons, no "leading" particle effect is present. Section 4 reviews the experimental evidence of the "leading" particle effect in hadron-hadron interactions; the experimental evidence for the same phenomenon in lepton-hadron interactions is given in Section 5. Conclusions are finally given in Section 6.

2. DEFINITION OF THE "LEADING" QUANTITY "L"

Consider the inclusive reaction

$$a + b \to c + \text{anything} \ . \qquad (1)$$

Particle c is a "leading" particle in reaction (1) if, on the average, it carries a sizeable fraction of the total energy available. The most convenient way of studying the "leading" particle effect in reaction (1) is therefore to use fractional energy or momentum variables, generally labelled by the symbol x.

Let E_c and $\vec{p}_c$ be the energy and momentum of particle c in the final state; E_{max} and $\vec{p}_{max}$ the kinematic bounds for E_c and $\vec{p}_c$ in reaction (1). The currently used fractional variables are x_F and x_R. The first variable has been introduced by Feynman,

$$x_F = p_L/p_{L,max} , \qquad -1 \leq x_F \leq 1 , \tag{2}$$

where p_L is the momentum component of particle c along the projectile direction in the centre-of-mass system for reaction (1); x_F ranges from -1 to +1, the negative values corresponding to the so-called target x-region, the positive values to the projectile x-region.

The radial variable x_R is the fractional energy defined according to

$$x_R = E_c/E_{max} , \qquad 0 \leq x_R \leq 1 . \tag{3}$$

For the sake of clarity, the type of x variable used will be explicitly indicated throughout the paper.

The inclusive single-particle cross-section integrated over p_T, used in this paper and referred to as F(x), is defined according to

$$F(x) = \frac{1}{\pi} \int \frac{2E_c}{\sqrt{s}} \frac{d^2\sigma}{dx dp_T^2} dp_T^2 , \tag{4}$$

where $\sqrt{s}$ is the total centre-of-mass energy.

In order to quantify the "leading" hadron effect, we have defined the following quantity:

$$L(x_0,x_1,x_2) = \frac{\int_{x_1}^{x_2} F(x)dx}{\int_{x_0}^{x_1} F(x)dx} , \tag{5}$$

where F(x) is the experimental invariant cross-section defined in Eq. (4). The ranges of x_F used are: $x_0 = 0.2$, $x_1 = 0.4$, $x_2 = 0.8$. They have been chosen in order to minimize the effect of the diffractive production ($x_F > 0.8$) and of the central production ($x_F < 0.2$).

3. HADRON PRODUCTION IN (e^+e^-) ANNIHILATION: NO "LEADING" HADRON EFFECT

The question we ask ourselves is: Given a certain amount of energy to be transformed into hadrons, does the produced multiparticle final-state system have a "leading" hadron? The answer comes from (e^+e^-) annihilation experiments: according to the experimental results obtained up to the highest energies studied so far, (e^+e^-) annihilation does not produce hadronic systems with a "leading" hadron. This is shown in the data reported below.

Figure 1a shows the inclusive cross-section $(s/\beta)(d\sigma/dx_R)$ versus $x_R = 2E/\sqrt{s}$ for $\pi^\pm$, $K^\pm$, and $\bar{p}$ measured at DORIS by the DASP Collaboration[15] at $\sqrt{s} = 5$ GeV. The experimental points for π, K, and $\bar{p}$ have the same x_R distribution, peaked at $x_R = 0$ and falling off steeply at a large value of x_R. No hadron shows a "leading" effect.

Figure 1b shows a compilation[16] of the inclusive cross-section $s(d\sigma/dx_p)$ versus $x_p = |\vec{p}|/|p_{beam}|$ for charged particles with $\sqrt{s}$ ranging from 5 to 30 GeV. The scaled cross-sections $(s/\beta)(d\sigma/dx)$ versus $x = 2E/W$ are shown for charged pions[17,18] in Fig. 1c, for charged and neutral kaons[17-19] in Fig. 1d, and for protons and antiprotons[18,20] in Fig. 1e. The distributions in Figs. 1c, 1d, and 1e are similar to the one in Fig. 1a. They all clearly show a trend that is opposite to the "leading" particle effect. This is quantitatively expressed by the values of L which are always below 0.5. A summary of all L values is shown in Table 1. The value of "L" has been calculated on the distributions of Fig. 1b because here the distributions extend to the highest x-values. It has then been assumed that these are the same for all particles. This assumption is justified by the fact that in the low x-region, where separate distributions are available, they all show a similar behaviour (Fig. 1a and Figs. 1c, d, e).

4. THE "LEADING" HADRON EFFECT IN PURELY HADRONIC INTERACTIONS

The following processes have been studied at ISR energies[21-24]:

$$\left.\begin{array}{ll}
[1] & pp \to p \ \ + \text{anything} \\
[2] & pp \to n \ \ + \text{anything} \\
[3] & pp \to \Lambda \ \ + \text{anything} \\
[4] & pp \to \Sigma^{+} + \text{anything} \\
[5] & pp \to \Sigma^{-} + \text{anything} \\
[6] & pp \to \bar{p} \ \ + \text{anything} \\
[7] & pp \to \bar{\Lambda} \ \ + \text{anything}
\end{array}\right\} \quad (A)$$

In order to compare these data with those at lower energy, we have studied the data taken on a fixed target (hydrogen) at incident proton momenta of 100 GeV/c. Moreover we have extended our study to other incident particles and even lower energies. This comparison is important for two reasons: i) it allows us to measure the energy dependence of the quantity "L"; ii) it allows us to see whether "L" varies when different hadrons are used (π, K, p, $\bar{p}$, etc.). The reactions investigated at 100 GeV/c are[25-29]:

$$\left.\begin{array}{ll}
[8] & pp \to p \ \ + \text{anything} \\
[9] & pp \to \bar{p} \ \ + \text{anything} \\
[10] & pp \to \pi^{+} + \text{anything} \\
[11] & pp \to \pi^{-} + \text{anything} \\
[12] & pp \to K^{+} + \text{anything} \\
[13] & pp \to K^{-} + \text{anything}
\end{array}\right\} \quad (B)$$

$$\left.\begin{array}{ll}
[14] & \bar{p}p \to \bar{p} \ \ + \text{anything} \\
[15] & \bar{p}p \to \pi^{+} + \text{anything} \\
[16] & \bar{p}p \to p \ \ + \text{anything}
\end{array}\right\} \quad (C)$$

$$\left.\begin{array}{ll} [17] & \pi^- p \to \pi^- + \text{anything} \\ [18] & \pi^- p \to \pi^+ + \text{anything} \\ [19] & \pi^- p \to p + \text{anything} \end{array}\right\} \text{(D)}$$

At 70 GeV/c of beam momentum the following reactions have been studied[30-31]:

$$\left.\begin{array}{ll} [20] & K^+ p \to c^+ + \text{anything} \\ [21] & K^+ p \to \pi^- + \text{anything} \\ [22] & K^+ p \to p + \text{anything} \end{array}\right\} \text{(E)}$$

(c^+ is a positively charged particle)

The following reactions

$$\left.\begin{array}{ll} [23] & K^- p \to \phi + \text{anything} \\ [24] & \pi^+ p \to \phi + \text{anything} \end{array}\right\} \text{(F)}$$

have been studied at even lower energies[32], i.e. at 10 and 16 GeV/c [reaction (23)] and 16 GeV/c [reaction (24)] K^- and π^+ momenta, respectively. Finally the following reactions[33-35]:

$$\left.\begin{array}{ll} [25] & \gamma p \to \rho + \text{anything} \\ [26] & \gamma p \to \omega + \text{anything} \\ [27] & \gamma p \to \phi + \text{anything} \end{array}\right\} \text{(G)}$$

have been investigated at incident photon momenta of 9.2 GeV/c for ρ and ω and 25.7 GeV/c for ϕ.

Reactions A and B are of the baryon-baryon type. Reactions C are of the antibaryon-baryon type. Reactions D, E, and F are of the meson-baryon type. In this latter class we include the (γp) processes [reactions (G)] because the "photon" is in fact a virtual vector meson and it allows us to extend our meson-baryon studies.

4.1 The energy dependence of the "leading" quantity "L"

A study of the quantity $L(x_0,x_1,x_2)$ versus the total c.m. energy of the colliding protons has been made, using Intersecting Storage Rings (ISR) data from $\sqrt{s}$ = 22 GeV to $\sqrt{s}$ = 53 GeV, for the inclusive neutron production[21]. No data are available for other hadrons in a wide energy range. This study shows that the quantity L, for the "neutron" case, scales. We have, however, pushed our study below the ISR energies, using Fermilab results at $\sqrt{s}$ = 13.7 GeV c.m. energy. Comparing proton data at $\sqrt{s}$ = 13.7 GeV with those at $\sqrt{s}$ = 62 GeV, the maximum variation of the quantity L is found to be ≃ 50%. However, this can be accounted for by strong variation of the "central" production of "protons" from Fermilab to ISR energies. This variation becomes very small in the ISR energy range. We will therefore assume that in the ISR energy range the quantity L scales for all types of hadrons.

4.2 Study of the quantity "L" using different hadrons

As the main purpose of this section is to study the "leading" effect versus different types of hadrons in the initial state, we will not include here the ISR results. The data obtained in (pp) collisions at ISR energies will be reported in Section 4.4. The main point to emphasize here is that the values of L for meson production at the ISR, i.e. in the highest energy (pp) collisions, compare well with the values obtained at 100 GeV/c.

4.2.1 Baryon-baryon collisions

As mentioned above, the baryon-baryon class is studied via the investigation of the multiparticle systems produced in proton-proton interactions at 100 GeV/c incident proton momentum[25] and at fixed p_T = 0.3 GeV/c. The data are shown in Fig. 2, where the invariant $E(d^3\sigma/dp^3)$ inclusive cross-section for the production of p, $\pi^\pm$, $K^\pm$, and $\bar{p}$ as a function of x_F is reported. Notice that the nominal centre-of-mass energy is $\sqrt{s}$ = 13.6 GeV. The x_F distributions for $\pi^\pm$, $K^\pm$, and $\bar{p}$ are peaked at x_F = 0, and decrease with increasing x_F values. The proton x_F distribution is very different: it is depressed at x_F = 0 and increases with increasing x_F. The value of the "leading" quantity L is $L_p \simeq 5$ for the proton; for all the other particles, L is an order of magnitude lower, $L \lesssim 0.5$, i.e. the proton is a "leading" particle in the final system of hadrons. The values of L are reported in Fig. 3. With increasing transverse momentum, the x_R distribution is still very different from the produced particles' distributions, as can be seen from Fig. 4 showing data from another spectrometer experiment[26]. In Fig. 4 the proton inclusive cross-section is plotted as a function of x_F for different values of p_T: from 0.25 to 1.5 GeV/c. The experimental points at large x_R can be fitted at all $p_T \geq 0.75$ GeV/c by the unique form $(1-x_R)^{0.5}$, as shown by the full lines in Fig. 4. The "leading" effect is clearly present also in the large-p_T domain.

4.2.2 Baryon-antibaryon collisions

Note that in (pp) interactions the baryonic number is B = 2 and it must be conserved. In order to establish if the "leading" effect has something to do with the value of B, we have studied at the same centre-of-mass energy, a reaction where B = 0, i.e. ($p\bar{p}$). Figure 5 shows data from a hydrogen bubble chamber experiments using 100 GeV/c antiprotons[27]. Here the invariant cross-sections F(x) are plotted as a function of x_F for π^+, p, and $\bar{p}$; backward π^- data have been averaged with the forward π^+ data. The antiproton x_F distribution has been determined, in the x_F range $0.4 \leq x_F \leq 1.0$, using the $d\sigma/dp_{lab}$ cross-section from the same experiment; it is, within errors, the reflection of the proton x_F distribution at negative x_F values. The produced pion x_F distribution is peaked at $x_F \approx 0$ and falls off at large x_F in about the same way as in (pp) interactions. As can be seen from the data, both the protons in the $x_F < 0$ region and the antiprotons in the $x_F > 0$ region show a "leading" behaviour. The values of L are in fact again an order of magnitude larger for $\bar{p}$ and p than those of the produced particles.

This shows that a hadronic system which starts with two baryons, behaves like the system which starts with a baryon-antibaryon pair. The "leading" particle effect is present in the same way in both cases. The data are reported in Fig. 6. For the produced pions the value of L is, as expected $L_\pi \lesssim 0.5$.

4.2.3 *Meson-baryon collisions*

Let us now consider interactions where the incident hadron is a meson instead of a baryon. Figure 7a shows, at 100 GeV/c π^- beam momentum, the π^+, π^-, and proton inclusive invariant x_F distributions integrated over p_T in (πp) interactions. The data are from the 30-inch hydrogen bubble chamber/wide-gap spark chamber hybrid system at Fermilab[28,29]. Here, both the proton and the π^- show a "leading" effect. The values of L for p and π^- are $L_p \geq 3$ and $L_{\pi^-} \simeq 2.5$, respectively. These results are shown in Fig. 8. The only difference between the "leading" baryon and the "leading" meson is that the latter is also produced abundantly at $x_F = 0$. Notice that the value of L for π^+ is, as expected for a particle which is produced without any "leading" effect: $L_{\pi^+} \simeq 0.5$ (see Fig. 8).

Figure 7b shows π^+ and π^- x_F distributions for (π^+p) interactions at 100 GeV/c. It can be clearly seen that the π^+ x_F distribution closely resembles the π^- x_F distribution of Fig. 7a. Both sets of data come from the same experiment[28] and can be directly compared: they show the same "leading" effect for π^+ and π^-. The value of L_{π^+} is in fact the same as the L_{π^-} mentioned above.

In Fig. 7c the (K^+p) data obtained at 70 GeV/c by the BEBC Collaboration[30,31] are presented. Here the K^+ are not resolved from the π^+. The x_F distribution of the positively charged particle c^+ must therefore be compared with that of the π^- and of the target proton. Although not resolved from π^+, the K^+ "leading" effect for $x_F > 0$ is clear. Also the target proton "leading" effect for $x_F < 0$ is equally clear. The values of L_{c^+} and of L_p are shown in Fig. 9.

Finally we turn to vector mesons. These are not available in hadron beams, but -- because of their J^{PC} quantum numbers -- they can be produced in photoproduction experiments. The reaction (γp) can therefore be regarded as a beam of ρ, ω, ϕ, and other vector mesons interacting with the proton. Figure 10 shows the x distribution of the vector mesons inclusively produced in the reaction

$$\gamma + p \to V + X \qquad (6)$$

The data are very limited; (ρ and ω) photoproduction were studied at 9.2 GeV, while ϕ photoproduction was studied at 25.7 GeV energy of incident photon. The data are from various photoproduction experiments[33-35]. The "leading" vector meson effect is clearly visible in the almost flat x distribution in the beam x-region $x_F > 0$. The values of L are shown in Fig. 11. Notice the anomalously large leading behaviour of the ω vector meson.

4.3 The "leading" effect when the incident particle does not change its nature

From this review it is evident that the "leading" effect is present in all hadron-hadron interactions. This effect should not be mistaken for the diffractive peak at x_F $(x_R) \simeq 1$. The "leading" hadron effect shows up in a very important x-range, typically from 0.2 to 0.8. This range is far enough away from the "central" production, $x \simeq 0$, and from the "peripherality" region, $x \simeq 1$. The initial-state hadron shows up in the final-state as a "leading" particle, with a nearly flat fractional energy or momentum distribution (x_F, x_R). Notice that the diffractive peak disappears for $p_T \gtrsim 0.7$ GeV/c, but the "leading" effect remains.

The "leading" effect seems naturally connected to the "quantum number flow" from the initial state to the particle in the final state. These quantum numbers -- flavour, J^{PC}, and colour -- are carried by the constituents which make up the initial-state hadron. The particle which carries more constituents of the initial state will have a sizeable fraction of the four-momentum of the initial state, and will hence appear to be "leading".

There is, however, a difference between mesons and baryons. Mesons show a "leading" effect and a sizeable central production. In fact the ratio

$$\frac{(d\sigma/dx)_{x=0}}{(d\sigma/dx)_{x\simeq 0.6}}$$

tends, for mesons, to be bigger than 1, whereas for baryons it is of the order of or smaller than 1. This can be naively explained by the simple fact that it is easier to produce a meson-antimeson than a baryon-antibaryon pair. In fact it is easier to recombine a quark-antiquark pair in order to obtain a meson, than three quarks (antiquarks) to obtain a baryon (antibaryon). In Fig. 12a we show, for comparison, the values of F(x) versus x_F of different hadron beams on a proton target. The fits are superimposed on the same figure so as to compare the shape in the $x_F > 0$ region. The curves are obtained from the data of Figs. 5, 7, and 10. For π^-, π^+, and K^+ mesons the contributions from centrally produced mesons have been subtracted. We have computed the value of the "leading" quantity "L" for the different beam particles excluding, as usual, the region below $x_F = 0.20$ (dominated by the central production) and above $x_F = 0.80$ (to eliminate diffractive production). The results are given in the first five rows of Table 2.

Figure 12b shows a comparison of the "leading" proton in the target x_F-region in reactions initiated by different beam particles. The corresponding "L" values, computed in the same x_F-region as discussed above, are reported in the last three rows of Table 2. These data show that no matter the nature of the incident particle, the proton keeps its "leading" effect, as expected.

Finally, for the (pp) case, the ISR results (which will be fully reported in the next section) show a clear "leading" effect.

So far, the "leading" effect has been studied when the incident particle goes from the initial state to the final state without changing its nature: a proton remains a proton, a π^+ remains a π^+, etc. In the next subsection we will consider the case where the incident particle changes its nature.

4.4 The "leading" effect when the incident particle changes its nature

What about the case of an incident hadron which transforms itself into another type of hadron? for example, a proton which becomes a Λ^0? There is definite evidence of the following fact: the "leading" phenomenon follows the rule that the "more similarity" there is (for example, in the sense of the quark content) between the hadronic particle observed in the final-state and the initial-state hadron, the more the "leading" effect is present. As mentioned in Section 2, the quantity "L" scales in the ISR energy range. Therefore the cleanest way of studying the "leading" effect when a hadron changes its nature, is to measure the quantity "L" for the various baryons produced in (pp) interactions at the ISR[21-24]. As discussed at the beginning of this section, the reactions investigated were:

$$\left.\begin{array}{ll} [1] & pp \to p + \text{anything} \\ [2] & pp \to n + \text{anything} \\ [3] & pp \to \Lambda + \text{anything} \\ [4] & pp \to \Sigma^+ + \text{anything} \\ [5] & pp \to \Sigma^- + \text{anything} \\ [6] & pp \to \bar{p} + \text{anything} \\ [7] & pp \to \bar{\Lambda} + \text{anything} \end{array}\right\}$$

Figure 13 shows the values of L for different hadrons produced in proton-proton collisions in the ISR energy range from 25 to 62 GeV. The dotted line is obtained using for L the functional form

$$F(x) = (1-x)^{2n-1} ,$$

where n is the number of quarks that need to be changed in order to give rise to the final wanted hadron[36-38]. This allows a comparison of our "leading" quantity L with old parametrization methods where the F(X) was parametrized as given above. The agreement is excellent. In Table 3 the values of L, shown in Fig. 13 are reported, together with the number of "propagating" quarks corresponding to the final-state hadron studied. In Fig. 13 the final states have been grouped according to the number of quarks propagating from the initial to the final state. For example, if we start with a proton, whose quark composition is (udu), and look at the Λ^0 whose quark composition is (uds), the propagating quarks are two (ud).

The results shown in Figs. 3, 6, 8 , and 9, 11, and 13, have a common trend, characterized by the number of propagating quarks: the value of L is the same when the number of propagating quarks is the same.

Recent studies on heavy-flavoured baryon production in (pp) collisions[10-14] clearly show the leading effect to be present also in Λ_c^+ and Λ_b^0 production.

The presence of the "leading" effect, connected to the number of propagating quarks, is clearly shown also by the investigation of reactions (F):

$$[23] \quad K^- p \to \phi + \text{anything}$$

$$[24] \quad \pi^+ p \to \phi + \text{anything} \; .$$

For reaction [23] the hadron in the final state, $\phi(s\bar{s})$, contains one of the quarks which make up the hadron in the initial state, $K^-(s\bar{u})$. Only one quark propagates in this case. For reaction [24] there is no quark propagation when going from a $\pi^+(u\bar{d})$ to a ϕ-meson $(s\bar{s})$. The data[32] of Fig. 14 clearly show a "leading" effect for the ϕ produced in reaction [23]. The value of L is $L_\phi \simeq 4.5$. The "leading" effect is not present in ϕ production from reaction [24], as expected. The value of L is $L_\phi \simeq 1$. It should be noticed that the value of L increases with decreasing energy of the incident hadron. This has a straightforward interpretation. At lower energy the "central" production is depressed. This produces a smaller denominator in our definition of L. The purpose of the analysis of reactions [23] and [24] was to see if even at this extreme low energy there was a clear difference in the L values for different numbers of propagating quarks.

5. THE "LEADING" HADRON IN LEPTON-HADRON COLLISIONS

In lepton-hadron ractions, i.e. (ep), (μp), and (νp) deep inelastic scattering, the energy available for hadron production is not the total centre-of-mass energy, but only the energy lost by the lepton. According to the standard formalism, we call (E-E′) the energy lost by the lepton, Q^2 the square of the four-momentum transfer (changed in sign), and W the invariant mass of the final-state hadronic system recoiling against the lepton.

Experimental results on the production of hadrons from (μp) deep inelastic scattering experiments and from high-energy (νp) interactions are at present available -- although not always with good particle identification. For our study, we have used data on hadron production in (νp) and ($\bar{\nu} p$) charged current events[39,40]. The data refer to exposures of the Fermilab 15 ft bubble chamber to broad-band ν and $\bar{\nu}$ beams. The x_F distributions of positive (h^+) and negative (h^-) hadrons are measured both in the forward and in the backward hemispheres. In the h^+ sample, protons can be identified, either by ionization or by kinematical fitting to the final states, and their x_F distribution can be derived. The most significant data refer to the reaction $\bar{\nu} p \to \mu^+ + p +$ anything, at $W \simeq 5$ GeV [40]. These are reported in Fig. 15. The h^+ distribution, as a function of x_F, shows a flat behaviour in the recoil hemisphere ($x_F < 0$), which is not present in the h^- case. Such an effect can be explained in terms of the presence of "leading" protons. In fact, for protons identified in the h^+ sample, the x_F distribution shows a plateau in the $x_F < 0$ region, thus providing direct evidence of the "leading" proton effect in ($\bar{\nu} p$) interactions. The value of L, derived from the data of Fig. 15, is $L_p = 3.2 \pm 0.5$. Similar features are shown by (νp) charged-current events, as described in Ref. 39.

The "leading" baryon effect is also present in the inclusive x_F distribution of the Λ^0 baryon produced both in electromagnetic and weak interactions. As we have seen in subsection 4.4, the Λ^0 is as "leading" as a baryon should be, when there are two propagating quarks. Figure 16 is a compilation[41] of production cross-sections of the Λ^0 in (ep), (νp), and ($\bar{\nu} p$) interactions: the x_F distributions have been normalized so as to compare their shape. The Λ^0 exhibits a clear "leading" effect in electromagnetic (ep) and weak (νp) and ($\bar{\nu} p$) interactions. The best data for measuring L_{Λ^0} are those for the reaction:

$$[28] \quad \bar{\nu} N \to \Lambda^0 + \text{anything} \, ,$$

referring to Fermilab 15 ft bubble chamber data at $W \simeq 4.5$ GeV. However, L_{Λ^0} can also be determined from data taken in a streamer chamber experiment at Cornell for the process:

[29] $ep \to \Lambda^0$ + anything ,

at the energy $W \simeq 3$ GeV. The values of L_{Λ^0} are reported in Fig. 17. As mentioned above, the data show that the "leading" effect in Λ^0 production is also present in electromagnetic and weak interactions, as first observed in purely hadronic interactions. In fact, the Λ^0 production corresponds to a proton which transforms into a Λ^0 via the propagation of two quarks. The value of L_{Λ^0} is as expected when the number of propagating quarks is two.

It is interesting to remark that also the energy dependence of L_{Λ^0} follows the trend already observed for the proton case (see subsection 4.1). At ISR energies, the value of L scales. At Fermilab energies, down to the energy of reaction [29], the behaviour of L can be summarized as follows: the lower is the energy available, the higher is the value of L.

6. CONCLUSIONS

Thanks to the use of the "leading" effect it has been possible to compare[1-9] the production of multihadron systems in (pp) interactions and (e^+e^-) annihilation. So far, the main trend had been that only high transverse momentum hadronic interactions could be a source of comparison with (e^+e^-) and deep inelastic scattering (DIS) in lepton-hadron physics. The use of the "leading" hadron effect has brought the vast amount of low-p_T physics into the very interesting domain of comparison with (e^+e^-) and DIS.

The study reported in the present paper shows that when a hadron interacts with another particle hadronically, electromagnetically, or weakly a very distinct feature emerges: the hadron, which is present in the initial state, keeps a privileged role in the energy sharing with the other hadrons produced. This distinctive feature is measured by the "leading" quantity "L". It is found that the value of this quantity is $L \sim 3$, when the number of propagating quarks is 3. If the number of propagating quarks is 2, the value of L is $L \simeq 1.5$. If only one quark propagates from the initial to the final state, the value of L is $L \simeq 0.5$. When there is no quark propagation from the initial to the final state, the particle produced has a value of the leading quantity, $L \simeq 0.2$. This value of L holds true, also, when a hadron is produced in (e^+e^-) annihilation. Here no hadron has a privileged energy-sharing, i.e. there is no "leading" hadron. In fact, in (e^+e^-) annihilation, in the initial state, there is a certain amount of energy E, to be used for the production of hadrons, but no hadron is present in the initial state.

For the "leading effect to show up, one needs an incoming hadron carrying good quantum numbers: colour, flavour, J^{PC}, etc. It is this quantum number "flow" which generates the "leading" phenomenon. Even when the incident particle changes its nature (for example, a proton becomes a neutron, or a Λ^0, or a Λ_c^+), i.e. when the initial-state quantum numbers are not fully carried by the final-state particle, the "leading" effect is still present.

The "leading" phenomenon therefore remains the cleanest effect, even in processes where quantum numbers become mixed and interchanged. Here we have a field of physics, the hadron constituents dynamics, which is far from being understood and is therefore difficult to take into account. In spite of all this, the "leading" effect shows up as a clear signature of simplifying unity.

For example, in deep-inelastic lepton-hadron scattering, the target hadron keeps a large fraction of the available energy. This is currently attributed to the gluons, but it is simply a "leading" baryon effect, whose significance in terms of gluons is a matter of theoretical speculation, as the quantum number "flow" mentioned above.

The use of the "leading" effect should be extended to the study of all hadronic phenomena. Its application to the analysis of multiparticle hadronic states produced in high-energy interactions will draw a more clear and more uniform picture in the study of processes induced by different particles at different energies.

REFERENCES

1) A. Zichichi, Evidence for a close link between (pp) and (e^+e^-) physics, in Proc. "Ettore Majorama" Int. School of Subnuclear Physics, 18th Course: The high-energy limit. (In press.)

2) M. Basile, G. Cara Romeo, L. Cifarelli, A. Contin, G. D'Ali, P. Di Cesare, B. Esposito, P. Giusti, T. Massam, F. Palmonari, G. Sartorelli, G. Valenti and A. Zichichi, Phys. Lett. 92B, 367 (1980).

3) M. Basile, G. Cara Romeo, L. Cifarelli, A. Contin, G. D'Ali, P. Di Cesare, B. Esposito, P. Giusti, T. Massam, R. Nania, F. Palmonari, G. Sartorelli, G. Valenti and A. Zichichi, Phys. Lett. 95B, 311 (1980).

4) M. Basile, G. Cara Romeo, L. Cifarelli, A. Contin, G. D'Ali, P. Di Cesare, B. Esposito, P. Giusti, T. Massam, R. Nania, F. Palmonari, G. Sartorelli, G. Valenti and A. Zichichi, Nuovo Cimento 58A, 193 (1980).

5) M. Basile, G. Cara Romeo, L. Cifarelli, A. Contin, G. D'Ali, P. Di Cesare, B. Esposito, P. Giusti, T. Massam, R. Nania, F. Palmonari, G. Sartorelli, G. Valenti and A. Zichichi, Nuovo Cimento Lett. 29, 491 (1980).).

6) M. Basile, G. Cara Romeo, L. Cifarelli, A. Contin, G. D'Ali, P. Di Cesare, B. Esposito, P. Giusti, T. Massam, R. Nania, F. Palmonari, G. Sartorelli, M. Spinetti, G. Susinno, G. Valenti and A. Zichichi, Phys. Lett. 99B, 247 (1981).

7) M. Basile, G. Cara Romeo, L. Cifarelli, A. Contin, G. D'Ali, P. Di Cesare, B. Esposito, P. Giusti, T. Massam, R. Nania, F. Palmonari, G. Sartorelli, M. Spinetti, G. Susinno, G. Valenti and A. Zichichi, Nuovo Cimento Lett. 30, 389 (1981).

8) M. Basile, G. Cara Romeo, L. Cifarelli, A. Contin, G. D'Ali, P. Di Cesare, B. Esposito, P. Giusti, T. Massam, R. Nania, F. Palmonari, G. Sartorelli, G. Valenti and A. Zichichi, Nuovo Cimento Lett. 30, 273 (1981).

9) M. Basile, G. Cara Romeo, L. Cifarelli, A. Contin, G. D'Ali, P. Di Cesare, B. Esposito, P. Giusti, G. Massam, R. Nania, F. Palmonari, V. Rossi, G. Sartorelli, M. Spinetti, G. Susinno, G. Valenti, L. Votano and A. Zichichi, charged particle multiplicities in (pp) interactions and comparison with (e^+e^-) data, preprint CERN EP/81-76, July 1981, Nuovo Cimento, in press.

10) M. Basile, G. Cara Romeo, L. Cifarelli, A. Contin, G. D'Ali, P. Di Cesare, B. Esposito, P. Giusti, T. Massam, F. Palmonari, G. Sartorelli, G. Valenti and A. Zichichi, Nuovo Cimento Lett. 30, 487 (1981).

11) M. Basile, G. Cara Romeo, L. Cifarelli, A. Contin, G. D'Ali, P. Di Cesare, B. Esposito, P. Giusti, T. Massam, F. Palmonari, G. Sartorelli, G. Valenti and A. Zichichi, Nuovo Cimento 63A, 230 (1981).

12) M. Basile, G. Bonvicini, G. Cara Romeo, L. Cifarelli, A. Contin, G. D'Ali, P. Di Cesare, B. Esposito, P. Giusti, T. Massam, R. Nania, F. Palmonari, G. Sartorelli, G. Valenti and A. Zichichi, Nuovo Cimento 31, 97 (1981).

13) M. Basile, G. Bonvicini, G. Cara Romeo, L. Cifarelli, A. Contin, G. D'Ali, P. Di Cesare, B. Esposito, P. Giusti, T. Massam, R. Nania, F. Palmonari, G. Sartorelli, G. Valenti and A. Zichichi. A comparison between "beauty" and "charm" production in (pp) interaction, preprint CERN-EP/81-75, July 1981, Nuovo Cimento, in press.

14) M. Basile, G. Bonvicini, G. Cara Romeo, L. Cifarelli, A. Contin, G. D'Ali, P. Di Cesare, B. Esposito, P. Giusti, T. Massam, R. Nania, F. Palmonari, G. Sartorelli, C. Valenti and A. Zichichi, The leading baryon effect in Λ_b production in proton-proton interactions at $\sqrt{s}$ = 62 GeV, preprint CERN-EP/81-72, July 1981, Nuovo Cimento, in press.

15) DASP Collaboration (R. Brandelik et al.), Phys. Lett. 67B, 358 (1977).

16) G. Wolf, DESY 80/13 (1980). Quoted data are taken from: i) DASP Collaboration (R. Brandelik et al.), Nucl. Phys. B148, 189 (1979); ii) G.J. Feldman and M.L. Perl, Phys. Rep. 33, 285 (1977); iii) TASSO Collaboration (R. Brandelik et al.), Phys. Lett. 89B, 418 (1980).

17) D. Pandoulas, Proc. 20th Int. Conf. on High-Energy Physics, Madison, Wis., 1980 (American Institute of Physics, New York, 1981), p. 596.

18) TASSO Collaboration (R. Brandelik et al.), Phys. Lett. 94B, 444 (1980).

19) V. Lüth, F.M. Pierre, G.S. Abrams, M.S. Alam, A.M. Boyarski, M. Breidenbach, W. Chinowsky, J. Dorfan, G.J. Feldman, G. Godlhaber, G. Hanson, J.A. Jaros, J.A. Kadyk, R.R. Larsen, A. Litke, D. Lüke, H.L. Lynch, R.J. Madaras, H.K. Nguyen, J.M. Paterson, M.L. Perl, I. Peruzzi, Ch. Peyrou, M. Piccolo, T.P. Pun, P. Rapidis, B. Richter, B. Sadoulet, R.H. Schindler, R.H. Schwitters, J. Siegrist, W. Tanenbaum. G.H. Trilling, F. Vanucci, J.S. Whitaker and J.E. Wiss, Phys. Lett. 70B, 120 (1977).

20) TASSO Collaboration (R. Brandelik et al.), Phys. Lett. 89B, 418 (1980).

21) J. Engler, B. Gibbard, W. Isenbeck, F. Mönning, J. Moritz, K. Pack, K.H. Schmidt, D. Wegener, W. Bartel, W. Flauger and H. Schopper, Nucl. Phys. B84, 70 (1975).

22) P. Capiluppi, G. Giacomelli, A.M. Rossi, G. Vanmini and A. Bussière, Nucl. Phys. B70, 1 (1974).

23) M.G. Albrow, A. Bagdius, D.P. Barber, A. Bogaerts, B. Bosnjakovic, J.R. Brooks, A.B. Clegg, F.C. Erne, C.N.P. Gee, D.H. Locke, F.K. Loebinger, P.G. Murphy, A. Rudge and J.C. Sens, Nucl. Phys. B73, 40 (1973).

24) S. Erhan, W. Lockman, T. Meyer, J. Rander, P. Schlein, R. Webb and J. Zsembery, Phys. Lett. 85B, 447 (1979).

25) A.E. Brenner, Proc. Seoul Symposium on Elementary Particles, Seoul, Korea, 1978 (Seoul National Univ., Korea, 1979), p. 709.

26) J.R. Johnson, R. Kammerud, T. Ohsugi, D.J. Ritchie, R. Shafer, D. Theriot, J.K. Walker and F.E. Taylor, Phys. Rev. D 17, 1292 (1978).

27) C.P. Ward, D.R. Ward, R.E. Ansorge, J.R. Carter, W.W. Neale, J.G. Rushbrooke, B.Y. Oh, M. Pratap, G.A. Smith, J. Whitmore, R. Raja and L. Voyvodic, Nucl. Phys. B153, 299 (1979).

28) J. Whitmore, B.Y. Oh, M. Pratap, G. Sionakides, G.A. Smith, V.E. Barnes, D.D. Carmony, R.S. Christian, A.F. Garfinkel, W.M. Morse, L.K. Rangan, L. Voyvodic, R. Walker, E.W. Anderson, H.B. Crawley, A. Firestone, W.J. Kernan, D.L. Parker, R.G. Glasser, D.G. Hill, M. Kazuno, G. McClellan, H.L. Price, B. Sechi-Zorn, G.A. Snow, F. Svreck, A.R. Erwin, E.H. Harvey, R.J. Loveless and M.A. Thompson, Phys. Rev. D 16, 3137 (1977).

29) P.D. Higgins, N.N. Biswas, J.M. Bishop, R.L. Bolduc, N.M. Cason, V.P. Kenney, R.C. Ruchti, W.D. Walker, J.S. Loos, L.R. Fortney, A.T. Goshaw, W.J. Robertson, E.W. Anderson, H.B. Crawley, A. Firestone, R. Floyd, W.J. Kernan, J.W. Lamsa, D.L. Parker, G.A. Snow, B.Y. Oh, M. Pratap, G. Sionakides, G.A. Smith, J. Whitmore, V. Sreedhar, G. Levman, B.M. Schwarzschild, T.S. Yoon, G. Hartner, P.M. Patel, L. Voyvodic and R.J. Walker, Phys. Rev. D 19, 731 (1979).

30) M. Barth, C. De Clercq, E.A. De Wolf, J.J. Dumont, D.P. Johnson, J. Lemonne, P. Peeters, R. Contri, H. Drevermann, L. Gerdyukov, Y. Goldschmidt-Clermont, G. Harigel, C. Milstene, J.P. Porte, R.T. Ross, P. Theocharopoulos, C. Caso, F. Fontanelli, R. Monge, S. Squarcia, U. Trevisan, J.F. Baland, J. Beaufays, J. Kesteman, F. Grard, P.A. van der Poel, L. Gatignon, W. Kittel, W.J. Metzger, D.J. Schotanus, A. Stergiou, R.T. Van de Walle, Y. Belokopitov, P.V. Chliapnikov, A. Fenuyk, V. Kubic, S. Lugovsky, S.G. Nikitin, V. Nikolaenko, Y. Petrovikh, V. Ronjin, O. Tchikilev and V. Yarba, Z. Phys. C 7, 183 (1981).

31) M. Barth, C. De Clercq, E. De Wolf, J.J. Dumont, D.P. Johnson, J. Lemonne, P. Peeters, R. Contri, H. Drevermann, L. Gerdyukov, Y. Goldschmidt-Clermont, G. Harigel, J. Joensuu, C. Milstene, J.P. Porte, R.T. Ross, M. Spyropoulou-Stassinaki, C. Caso, F. Fontanelli, R. Monge, S. Squarcia, U. Trevisan, J.F. Baland, J. Beaufays, F. Grard, J. Hanton, P.A. Van der Poel, L. Gatignon, W. Kittel, W.J. Metzger, D.J. Schotanus, A. Stergiou, R.T. Van de Walle, Y. Belokopitov, B. Brizgalov, P. Chliapnikov, A. Fenuyk, V. Kubic, E. Krytchenko, S. Lugovsky, V. Nikolaenko, J. Petrovik, V. Ronjin, O. Tchikilev, V. Yarba and V. Zjigunov, Z. Phys. C 7, 89 (1981).

32) D.R.O. Morrison, Preprint CERN-EP/79-102 (1979) and references therein.

33) C.A. Nelson, Jr., E.N. May, J. Abramson, D.E. Andrews, J. Harvey, F. Lobkowicz, M.N. Singer, E.H. Thorndike and M.E. Nordberg, Jr., Phys. Rev. D 17, 647 (1978).

34) E. Kogan, J. Ballam. G.B. Chadwick, K.C. Moffeit, P. Seyboth, I.O. Skillicorn, H. Spitzer, G. Wolf, H.H. Bingham, W.B. Fretter, W.J. Podolsky, M.S. Rabin, A.H. Rosenfeld, G. Smadja and Y. Eisenberg, Nucl. Phys. B122, 383 (1977).

35) D. Aston, M. Atkinson, R. Bailey, A.H. Ball, B. Bouquet, G.R. Brookes, J. Bröring, P.J. Bussey, D. Clarke, A.B. Clegg, B. d'Almagne, G. de Rosny, B. Diekmann, A. Donnachie, M. Draper, B. Drevillon, I.P. Duerdoth, J.-P. Dufey, R.J. Ellison, D. Ezra, P. Feller, A. Ferrer, P.J. Flynn, F. Friese, W. Galbraith, R. George, S.D.M. Gill, M. Goldberg, S. Goodman, W. Graves, B. Grossetête, P.G. Hampson, K. Heinloth, R.E. Hughes-Jones, J.S. Hutton, M. Ibbotson, M. Jung, S. Katsanevas, M.A.R. Kemp, F. Kovacs, B.R. Kumar, G.D. Lafferty, J.B. Lane, J.-M. Lévy, V. Liebenau, J. Litt, G. London, D. Mercer, J.V. Morris, K. Müller, D. Newton, E. Paul, P. Petroff, Y. Pons, C. Raine, F. Richard, R. Richter, J.H.C. Roberts, P. Roudeau, A. Rougé, M. Sené, J. Six, I.O. Skillicorn, J.C. Sleeman, K.M. Smith, C. Steinhauer, K.M. Storr, D. Treille, Ch. de la Vaissière, H. Videau, I. Videau, A.P. Waite, A. Wijangco, W. Wojcik, J.-P. Wuthrick and T.P. Yiou, preprint CERN-EP/80-181 (1980).

36) D. Denegri, C. Cochet, M.A. Jabiol, C. Lewin, L. Mosca, M.L. Faccini-Turluer, D. Vilanova, L. Becker, U. Gensch, M. Barth, E.A. de Wolf, M. Gysen, M. Van Immerseel, C. Poiret, R. Windmolders, I.V. Ajinenko, Yu. Arestov, A.A. Borovikov, P.V. Chliapnikov, V.V. Kniazev, E.A. Kozlovsky, M.N. Ukhanov, E.V. Vlasov, H. Dibon and M. Markytan, Phys. Lett. 98B, 127 (1981), and references therein.

37) D. Cutts, R.S. Dulude, R.E. Lanou, Jr., J.T. Massimo, R. Meunier, A.E. Brenner, D.C. Carey, J.E. Elias, P.H. Garbincius, G. Mikenberg, V.A. Polychronakos, M.D. Chiaratia, C. DeMarzo, C. Favuzzi, G. Germinario, L. Guerriero, P. LaVopa, G. Maggi, F. Posa, G. Selvaggi, P. Spinelli, F. Waldner, W. Aitkenhead, D.S. Barton, G.W. Brandenburg, W. Busza, T. Dobrowolski, J.I. Friedman, H.W. Kendall, T. Lyons, B. Nelson, L. Rosenson, W. Toy, R. Verdier and L. Votta, Phys. Rev. Lett. 43, 319 (1979).

38) J.S. Gunion, Phys. Lett. 88B, 150 (1979).

39) J. Bell, C.T. Coffin, R.N. Diamond, H.T. French, W.C. Louis, B.P. Roe, R.T. Ross, A.A. Seidl, J.C. Vander Velde, E. Wang, J.P. Berge, D.V. Bogert, F.A. DiBianca, R. Endorf, R. Hanft, C. Kochowski, J.A. Malko, G.I. Moffatt, F.A. Nezrick, W.G. Scott, W. Smart, R.J. Cence, F.A. Harris, M. Jones, M.W. Peters, V.Z. Peterson, V.J. Stenger, G.R. Lynch, J.P. Marriner and M.L. Stevenson, Phys. Rev. D 19, 1 (1979).

40) M. Derrick, P. Gregory, F. LoPinto, B. Musgrave, J. Schlereth, P. Schreiner, R. Singer, S.J. Barish, R. Brock, A. Engler, T. Kikuchi, R.W. Kraemer, F. Messing, B.J. Stacey, M. Tabak, V.E. Barnes, T.S. Carman, D.D. Carmony, E. Fernandez, A.F. Garfinkel and A.T. Laasanen, preprint ANL-HEP-PR-80-54 (1980).

41) V. Ammosov, A. Amrakhov, A. Denisov, P. Ermolov, V. Gapienko, V. Klyukhin, V. Koreshev, P. Pitukhin, V. Sirotenko, E. Slobodyuk, V. Zaetz, J.P. Berge, D. Bogert, R. Hanft, J. Malko, G. Harigel, G. Moffatt, F. Nezrick, J. Wolfson, V. Efremenko, A. Fedotov, P. Gorichev, V. Kaftanov, G. Kliger, V. Kolganov, S. Krutchinin, M. Kubantsev, I. Makhlyueva, V. Shekeljan, V. Shevchenko, J. Bell, C.T. Coffin, W. Louis, B.P. Roe, R.T. Ross, D. Sinclair and E. Wang, Nucl. Phys. B162, 205 (1980), and references therein.

Table 1

Value of the "leading" quantity "L" measured for various types of hadrons, i.e. π^+, π^-, K^+, K^-, p, $\bar{p}$, produced in e^+e^- interactions

Reaction	"L"
$e^+e^- \to \pi^+$ + any	0.16 ± 0.03
$e^+e^- \to \pi^-$ + any	0.16 ± 0.03
$e^+e^- \to K^+$ + any	0.16 ± 0.03
$e^+e^- \to K^-$ + any	0.16 ± 0.03
$e^+e^- \to p$ + any	0.16 ± 0.03
$e^+e^- \to \bar{p}$ + any	0.16 ± 0.03

Table 2

Value of the "leading" quantity "L" measured for various types of hadron beams, i.e. π^+, π^-, K^+, p, $\bar{p}$

Reaction	x_F region	"L"
$\pi^+p \to \pi^+$ + any	> 0	2.5 ± 0.3
$\pi^-p \to \pi^-$ + any	> 0	2.5 ± 0.3
$K^+p \to K^+$ + any	> 0	1.5 ± 0.2
$pp \to p$ + any	> 0	5 ± 0.5
$\bar{p}p \to \bar{p}$ + any	> 0	4.5 ± 0.5
$\bar{p}p \to p$ + any	< 0	4 ± 0.5
$K^+p \to p$ + any	< 0	4 ± 0.5
$\pi^-p \to p$ + any	< 0	3 ± 0.4

Table 3

ISR (pp) processes

Initial state: proton (udu)			
Final state particle	Quark composition	Propagating quarks	L
p	(udu)	(udu)	3.2 ± 0.2
n	(udd)	(ud)	1.92 ± 0.05
Λ^0	(uds)	(ud)	1.02 ± 0.10
Σ^+	(usu)	(uu)	1.15 ± 0.17
Σ^-	(dds)	(d)	0.53 ± 0.15
$\bar{p}$	($\bar{u}\bar{d}\bar{u}$)	nothing	0.30 ± 0.05
$\bar{\Lambda}^0$	($\bar{u}\bar{s}\bar{d}$)	nothing	0.10 ± 0.02

Figure captions

Fig. 1 : Inclusive production of hadrons in (e^+e^-) annihilation.

a) The cross-section $(s/\beta)(d\sigma/dx_R)$ versus x_R for $(\pi^+ + \pi^-)$, $(K^+ + K^-)$ and twice the $\bar{p}$ yield for $\sqrt{s} = 5$ GeV (Ref. 15).

b) The cross-section $s(d\sigma/dx_p)$ for inclusive charged particle production measured at energies of 5 to 30 GeV (Ref. 16).

c) The scaled cross-section $(s/\beta)d\sigma/dx$ for charged pions (Refs. 17,18).

d) The scaled cross-section $(s/\beta)d\sigma/dx$ for neutral and charged kaons (Refs. 17-19). The average pion cross-section is shown as the solid curve.

e) The scaled cross-section $(s/\beta)d\sigma/dx$ for protons and antiprotons (Refs. 18,20). The average charged pion cross-section is shown as the solid curve.

Fig. 2 : Inclusive production of hadrons in (pp) interactions. The invariant cross-section $E(d^3\sigma/dp^3)$ at 100 GeV/c as a function of x_F at fixed $p_T = 0.3$ GeV/c, for p, $\pi^\pm$, $K^\pm$, and $\bar{p}$ (Ref. 25).

Fig. 3 : L(0.2, 0.4, 0.8) for various final-state hadrons produced in pp collisions at $P_{lab} = 100$ GeV/c.

Fig. 4 : Inclusive production of hadrons in (pp) interactions. The invariant cross-section $E(d^3\sigma/dp^3)$ at 100 GeV/c as a function of x_R at various p_T from 0.25 to 1.5 GeV/c for protons (Ref. 26). Open triangles at $p_T = 1.25$ GeV/c are data at 400 GeV/c. The dotted lines on the figure are hand-drawn to guide the eye through the data points; the full line is the shape of $(1-x)^{0.5}$ functional behaviour.

Fig. 5 : Inclusive production of hadrons in $(p\bar{p})$ interactions. Invariant cross-section integrated over p_T as a function of x_F for π^+, p, and $\bar{p}$ as measured in 100 GeV/c $\bar{p}$ interactions in a hydrogen bubble chamber. (Data from Ref. 27.)

Fig. 6 : L(0.2, 0.4, 0.8) for final-state hadrons produced in $\bar{p}$-p collisions at $P_{lab} = 100$ GeV/c.

Fig. 7 : Inclusive production of hadrons in (πp) and (Kp) interactions.

a) Invariant cross-section integrated over p_T as a function of x_F for π^+, π^-, and p as measured in 100 GeV/c (π^-p) interactions in a hydrogen bubble chamber. (Data from Refs. 28 and 29.)

b) The same as for (a) using 100 GeV/c (π^+p) interactions. (Data from Ref. 28.)

c) Invariant cross-section at fixed p_T = 0.3 GeV/c as a function of x_F for inclusive production in (K^+p) interactions at 70 GeV/c in BEBC. (Data from Refs. 30 and 31.) Shown is the x_F distribution of positively charged mesons c^+ (slow protons subtracted), of π^-, and of the target protons.

Fig. 8 : L(0.2, 0.4, 0.8) for final-state hadrons produced in π^-p at P_{lab} = 100 GeV/c.

Fig. 9 : L(0.2, 0.4, 0.8) for final-state hadrons produced in $K^{\pm}$p at P_{lab} = 100 GeV/c.

Fig. 10 : Inclusive x_F distribution of vector mesons in (γp) interactions: ρ meson (Ref. 33) and ω meson (Ref. 34) at γ energy of 9.2 GeV. The ϕ-meson distribution (plotted with arbitrary normalization from Ref. 35) is for a γ energy of 25.70 GeV.

Fig. 11 : L(0.2, 0.4, 0.8) for final-state vector mesons produced in γp.

Fig. 12 : a) x_F distribution in the beam x_F-region (x_F > 0) for $\pi^{\pm}$, K, and $\bar{p}$ incident particles on the target protons.

b) x_F distribution for the target proton in the reactions (πp), (Kp), ($\bar{p}$p).

Fig. 13 : The leading quantity L(0.2, 0.4, 0.8) for various final state hadrons in pp collisions at ISR energies (25 - 62 GeV) is plotted versus the number of propagating quarks from the incoming into the final-state hadrons. The dotted line is obtained by using a parametrization of the single particle inclusive cross-section, as described in the text.

Fig. 14 : Centre-of-mass x_F distribution for inclusive production of ϕ-mesons in K^-p and π^+p interactions (Ref. 32).

Fig. 15 : Inclusive production of hadrons in ($\bar{\nu}$p) charged-current interactions. The centre-of-mass x_F distributions for positive-charge particles (h^+), for negative-charge particles (h^-), and for identified protons (Ref. 40).

Fig. 16 : Inclusive production of the Λ^0 baryon in (νp), ($\bar{\nu}$p), and (ep) interactions. Data from Ref. 41 are normalized to the same cross-section.

Fig. 17 : L(0.2, 0.4, 0.8) for Λ^0 productions in ($\bar{\nu}$p) and (ep) reactions. The dotted line is the same as described for Fig. 13.

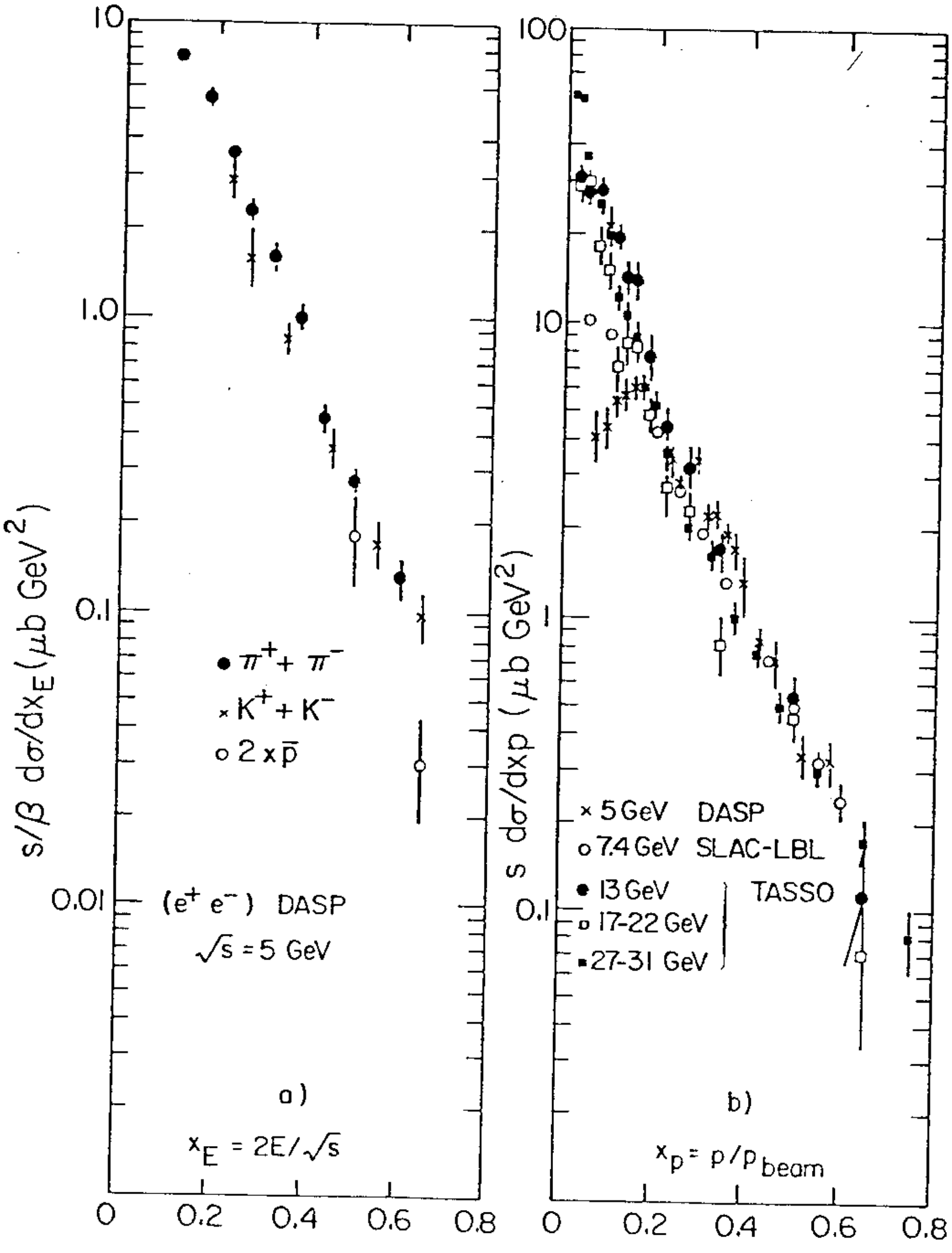

s/β dσ/dx_E (μb GeV^2)
π+ + π−
K+ + K−
2 x p̄
(e+ e−) DASP
√s = 5 GeV
a)
x_E = 2E/√s
s dσ/dxp (μb GeV^2)
5 GeV DASP
7.4 GeV SLAC-LBL
13 GeV
17-22 GeV
27-31 GeV
TASSO
b)
x_p = p/p_beam

Fig. 1 a) b)

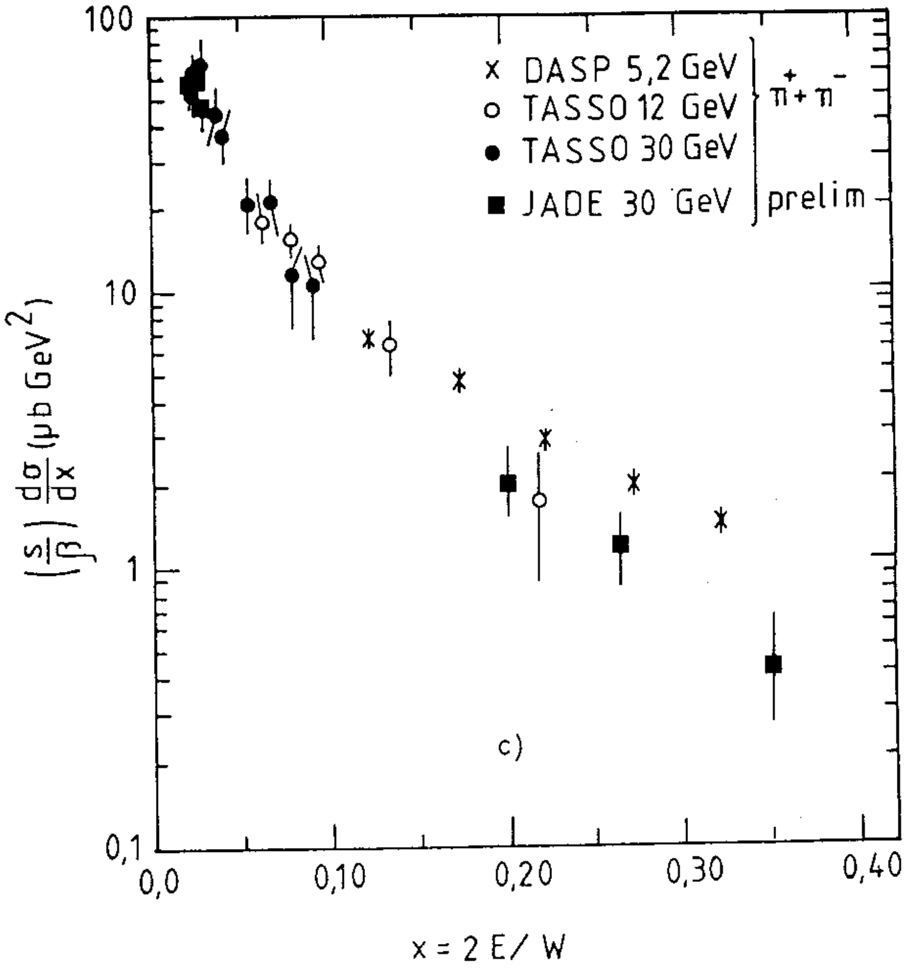

100
10
1
0,1
0,0
0,10
0,20
0,30
0,40
$\left(\frac{s}{\beta}\right)\frac{d\sigma}{dx}$ (μb GeV^2)
x = 2 E/ W
x DASP 5,2 GeV
o TASSO 12 GeV
● TASSO 30 GeV
■ JADE 30 GeV
$\pi^+ + \pi^-$
prelim
c)

Fig. 1 c)

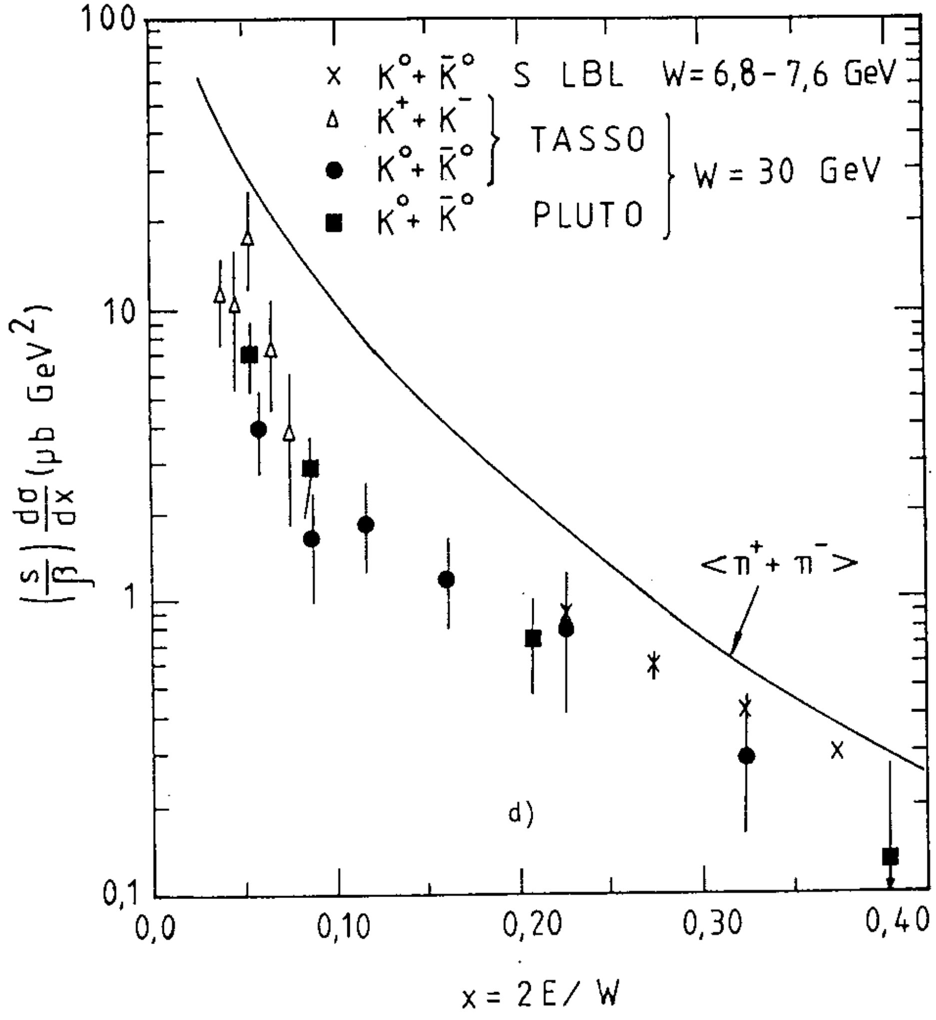

100
10
1
0,1
0,0
0,10
0,20
0,30
0,40
$\left(\frac{s}{\beta}\right)\frac{d\sigma}{dx}$ (μb GeV^2)
x = 2 E/ W
x $K^o + \bar{K}^o$ S LBL W = 6,8 - 7,6 GeV
Δ $K^+ + K^-$
● $K^o + \bar{K}^o$
TASSO
■ $K^o + \bar{K}^o$ PLUTO
W = 30 GeV
$<\pi^+ + \pi^->$
d)

Fig. 1 d)

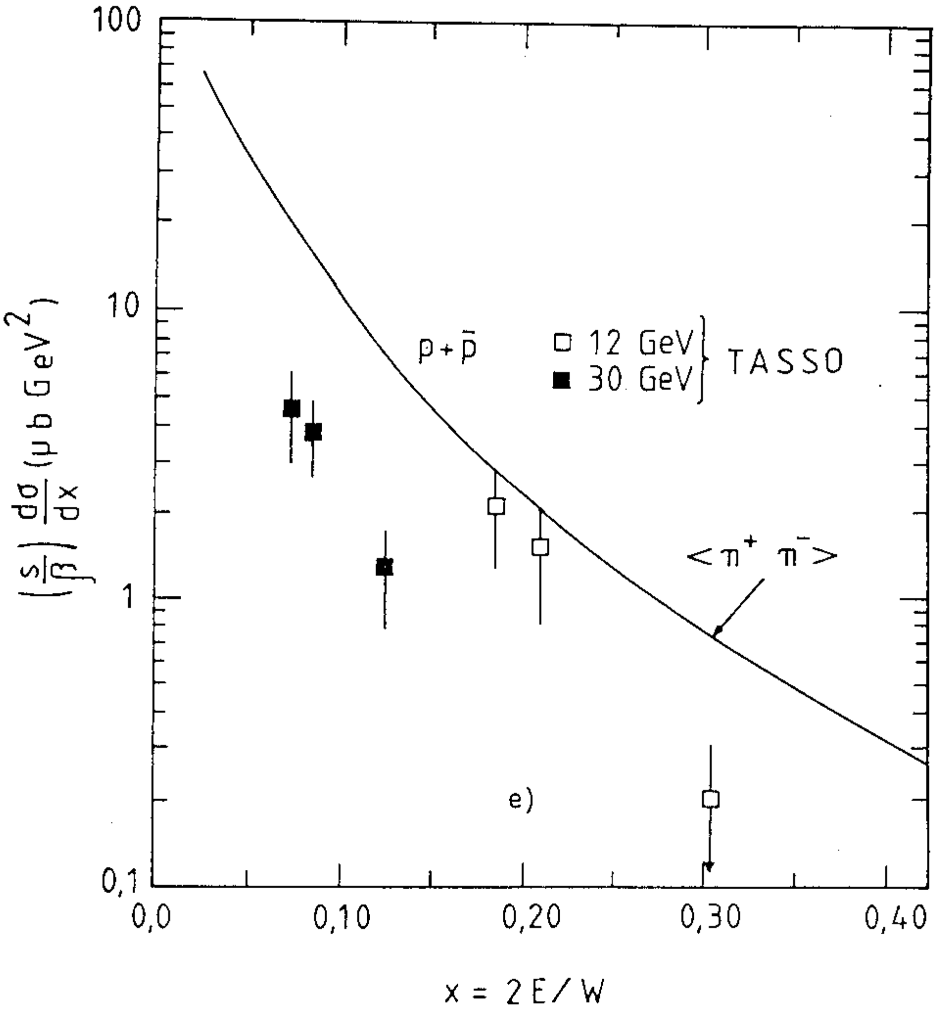

100
10
1
0,1
0,0
0,10
0,20
0,30
0,40
$(\frac{s}{\beta})\ \frac{d\sigma}{dx}$ (μb GeV²)
x = 2E/W
p + p̄
12 GeV
30 GeV
TASSO
<π⁺ π⁻>
e)

Fig. 1 e)

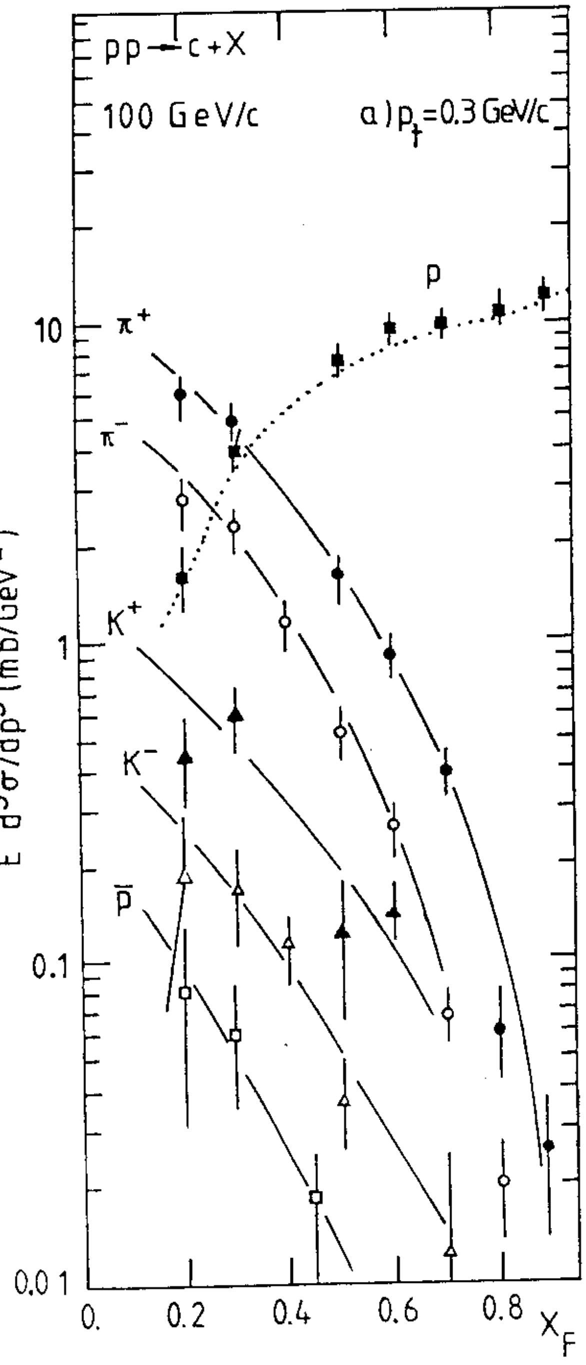
pp → c+X
100 GeV/c
a) p_t=0.3 GeV/c
p
π^+
π^-
K^+
K^-
$\bar{p}$
E $d^3\sigma/dp^3$ (mb/GeV^2)
10
1
0.1
0.01
0.
0.2
0.4
0.6
0.8
X_F

Fig. 2

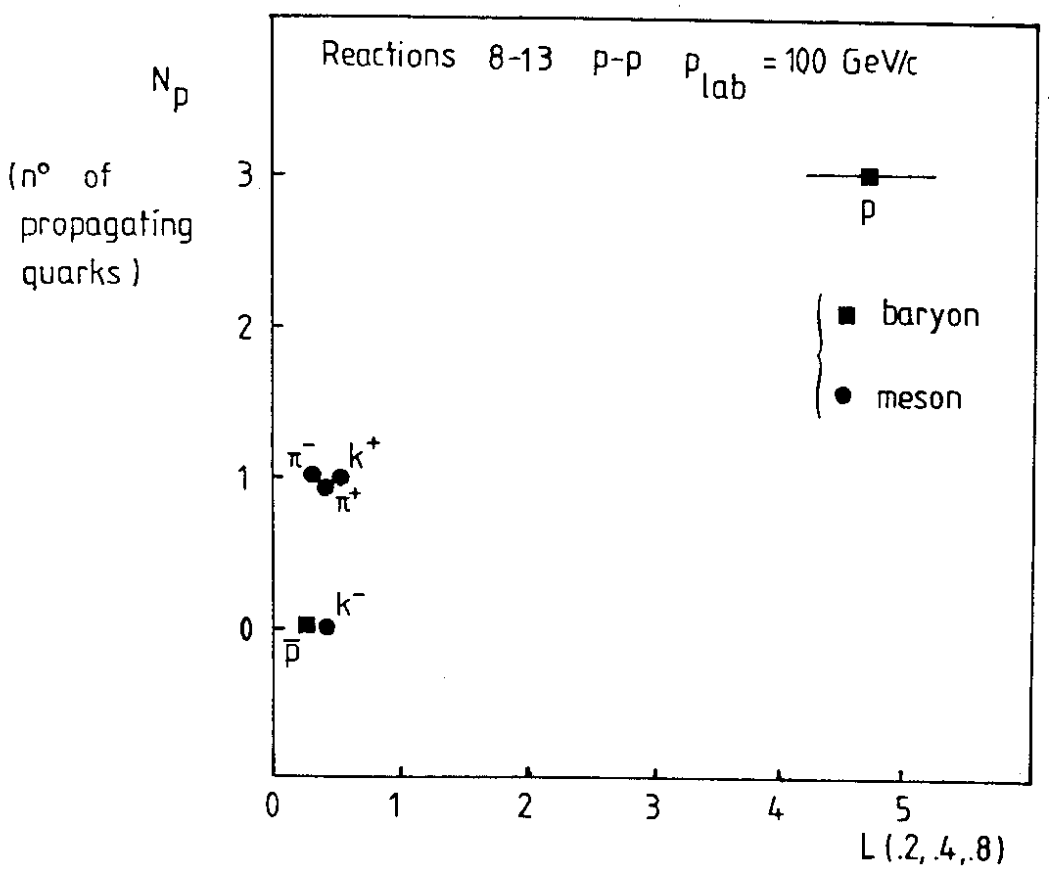

Reactions 8-13 p-p P_{lab} = 100 GeV/c
N_p
(n° of propagating quarks)
3
2
1
0
p
baryon
meson
π⁻
k⁺
π⁺
k⁻
p̄
0
1
2
3
4
5
L (.2, .4, .8)

Fig. 3

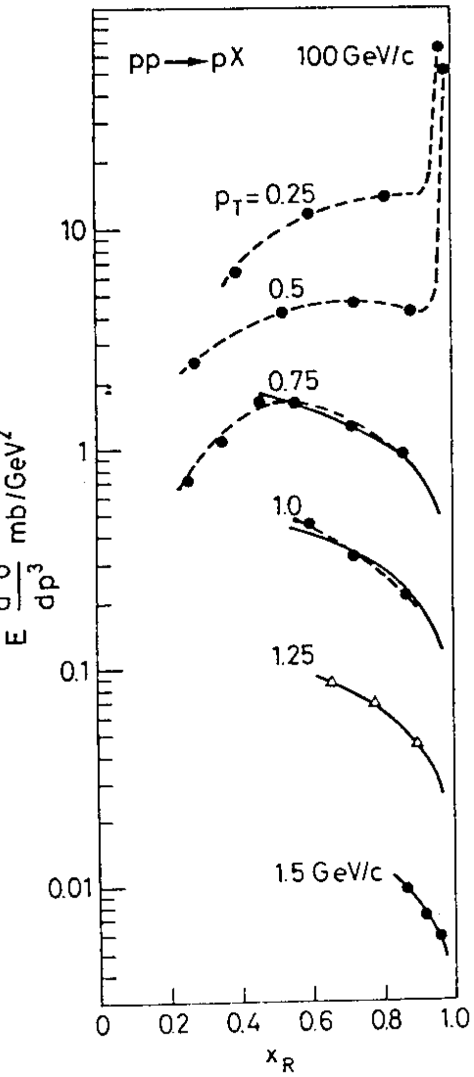

pp → pX
100 GeV/c
p_T = 0.25
0.5
0.75
1.0
1.25
1.5 GeV/c
$E \frac{d^3\sigma}{dp^3}$ mb/GeV^2
x_R

Fig. 4

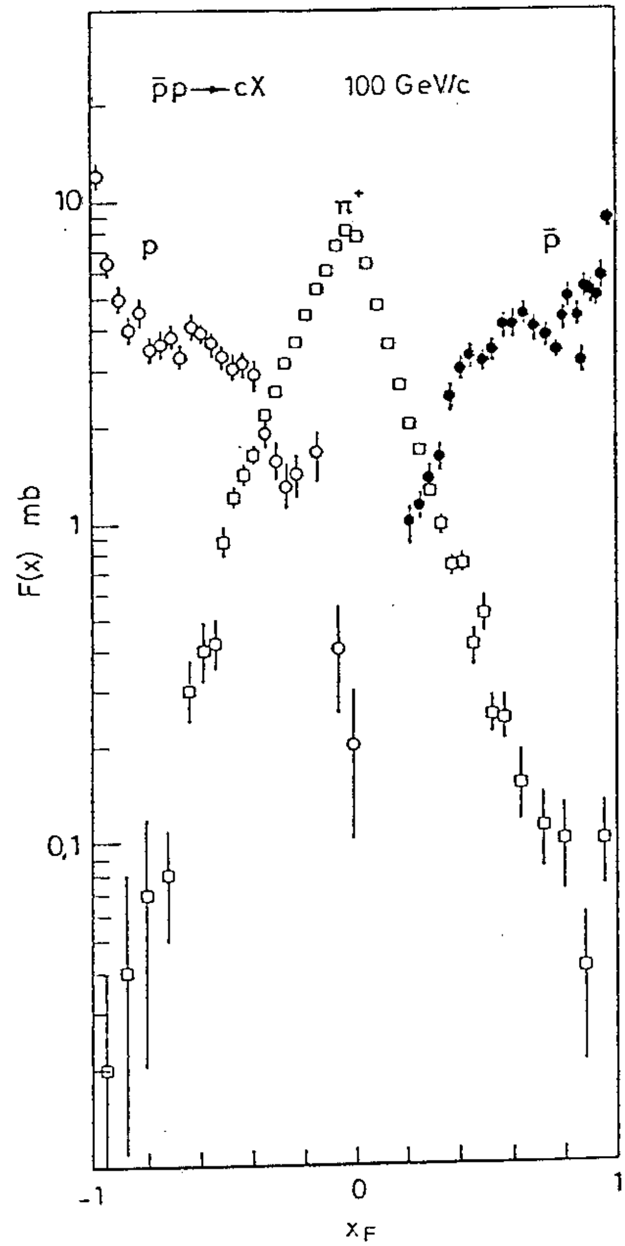

p̄p → cX
100 GeV/c
p
π⁺
p̄
F(x) mb
x_F

Fig. 5

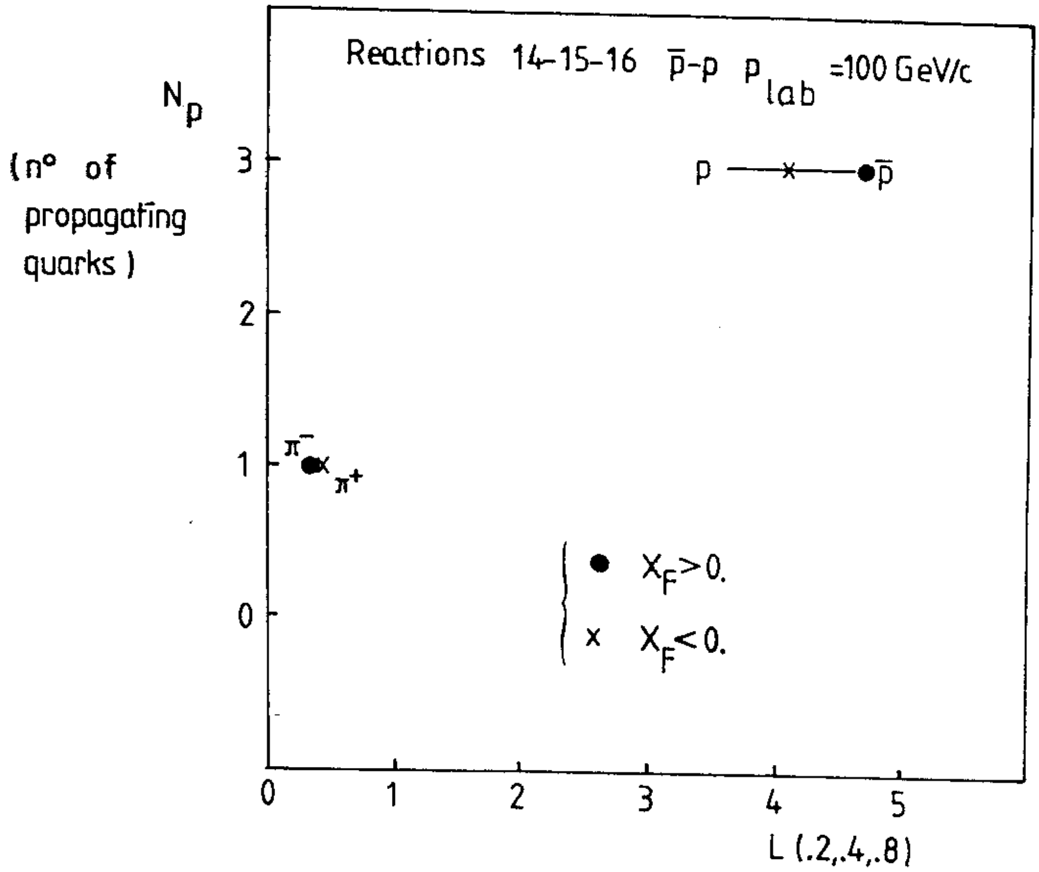

Reactions 14-15-16 p̄-p p_{lab} =100 GeV/c
N_p
(n° of propagating quarks)
3
2
1
0
p
p̄
π⁻
π⁺
● X_F>0.
× X_F<0.
0
1
2
3
4
5
L (.2,.4,.8)

Fig. 6

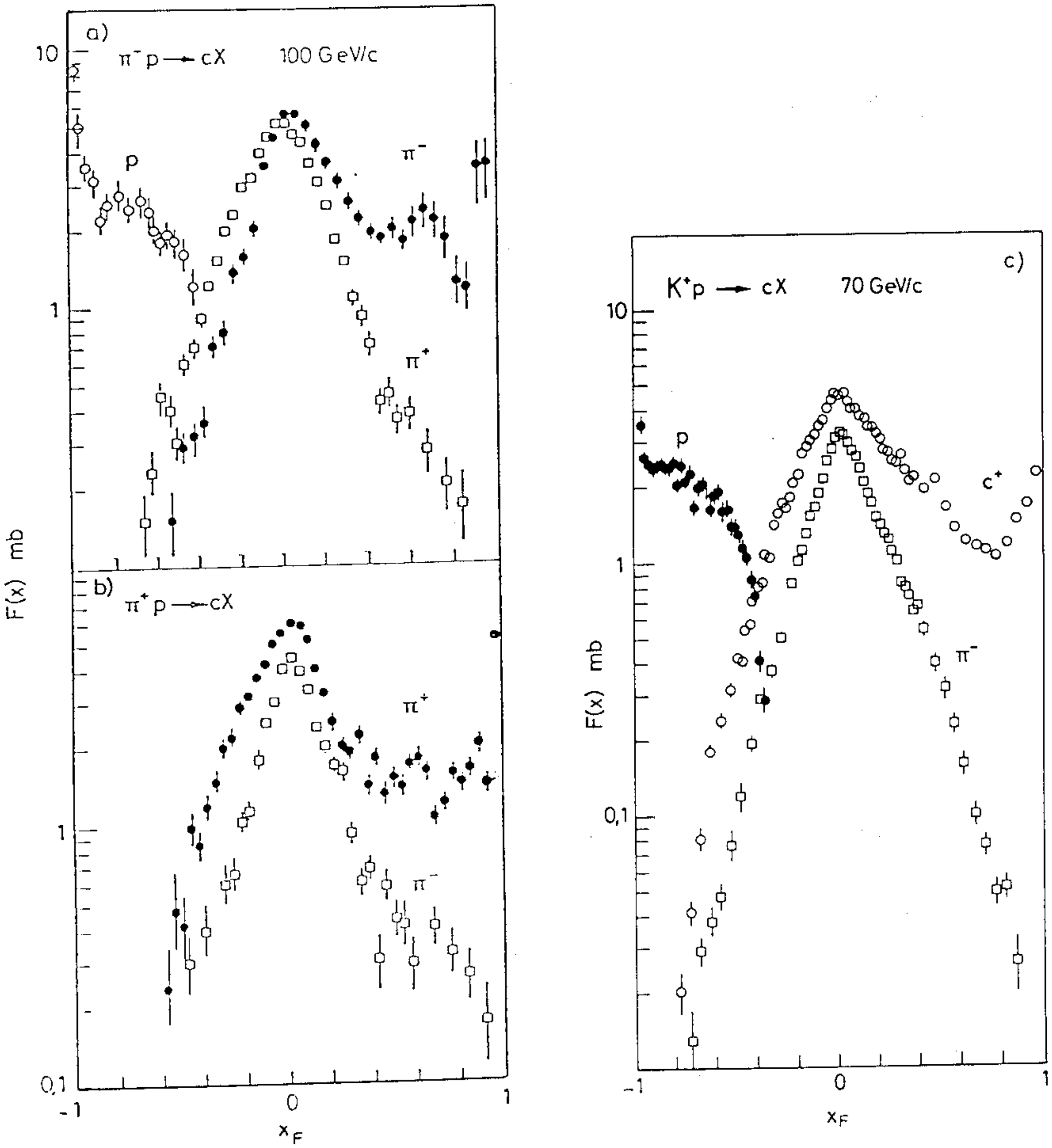

Fig. 7

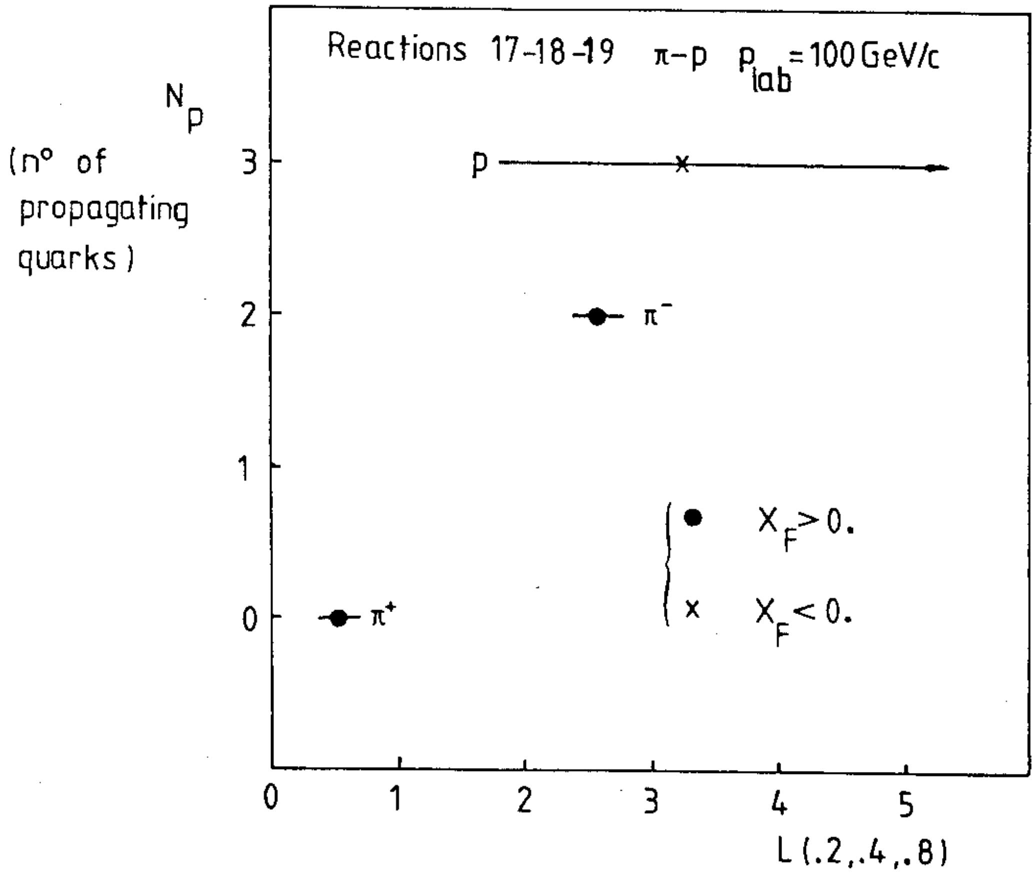
Reactions 17-18-19 π-p p_{lab}=100 GeV/c
N_p
(n° of
propagating
quarks)
3
2
1
0
p
π^-
π^+
$X_F > 0.$
$X_F < 0.$
0
1
2
3
4
5
L(.2,.4,.8)

Fig. 8

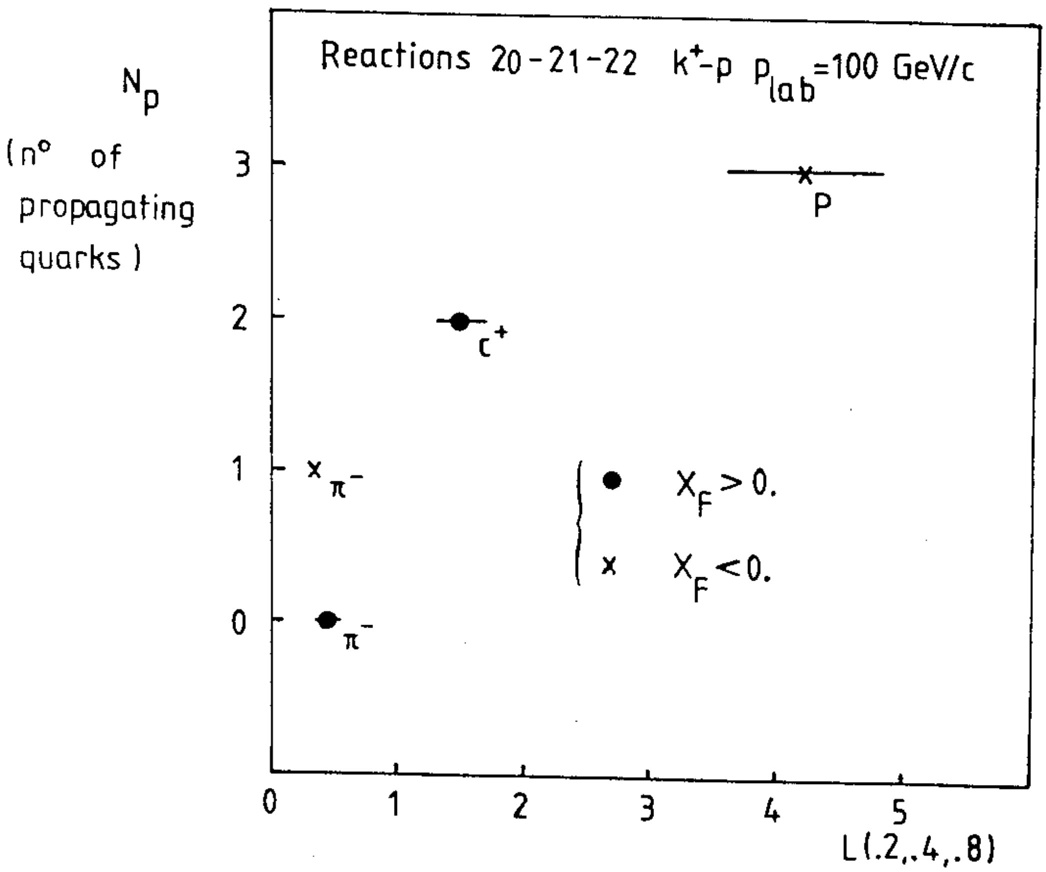
Reactions 20-21-22 k^+-p p_{lab}=100 GeV/c
N_p
(n° of
propagating
quarks)
3
2
1
0
P
c^+
π^-
π^-
$X_F > 0.$
$X_F < 0.$
0
1
2
3
4
5
L(.2,.4,.8)

Fig. 9

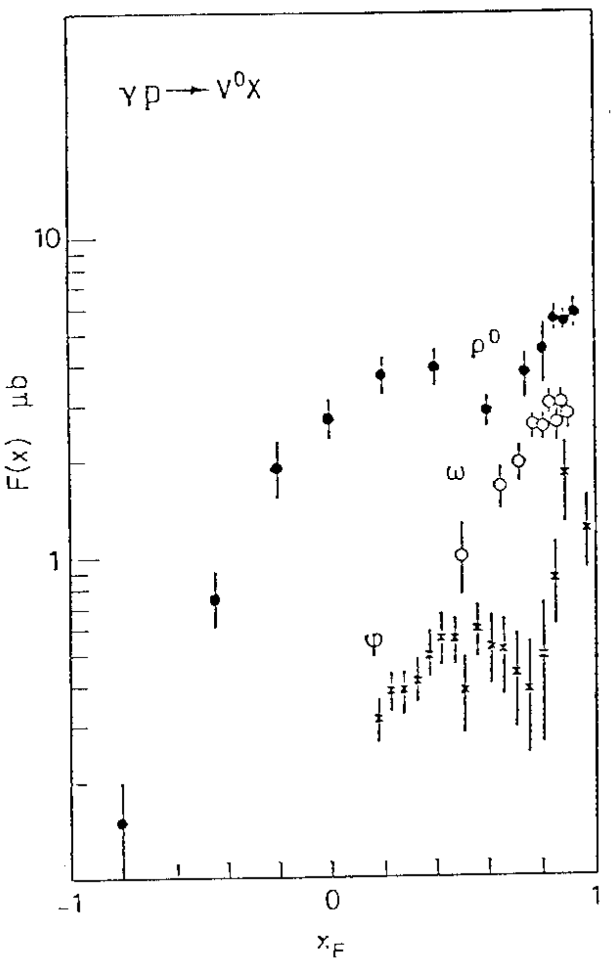

γ p → V⁰X
10
1
F(x) μb
ρ⁰
ω
φ
-1
0
1
x_F

Fig. 10

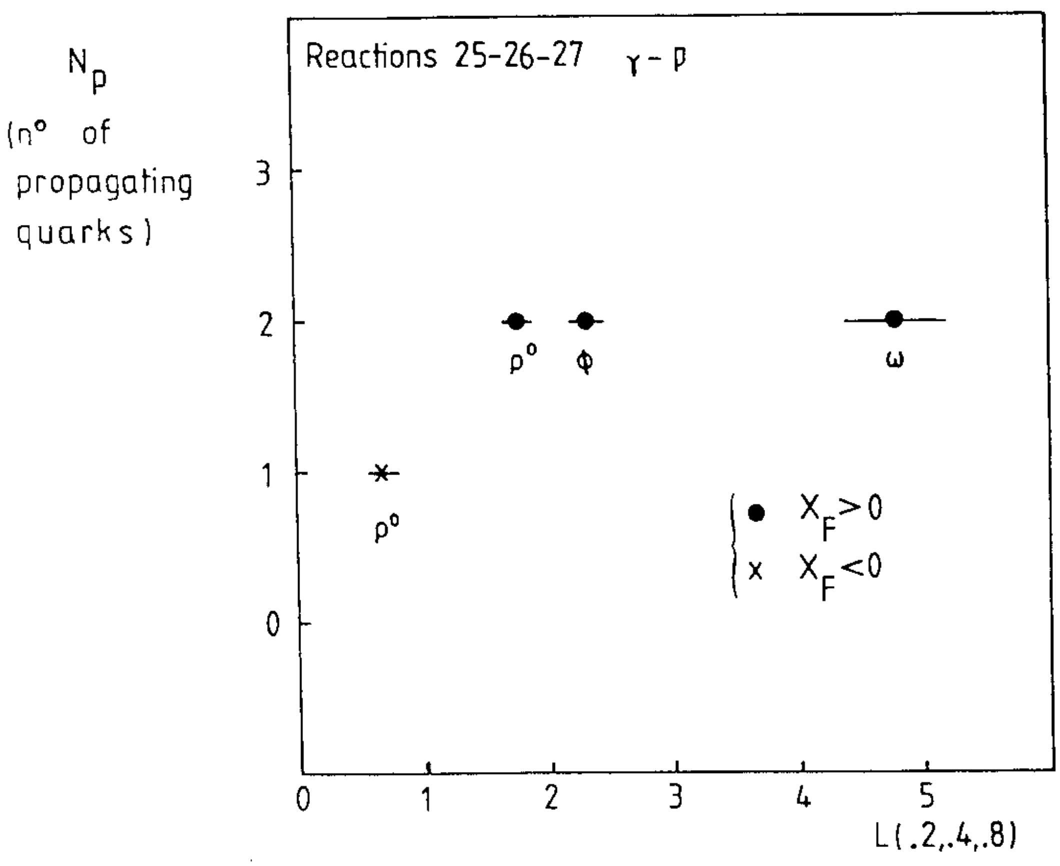

N_p
(n° of propagating quarks)
Reactions 25-26-27 γ - p
3
2
1
0
ρ⁰
φ
ω
ρ⁰
● $X_F > 0$
x $X_F < 0$
0
1
2
3
4
5
L(.2,.4,.8)

Fig. 11

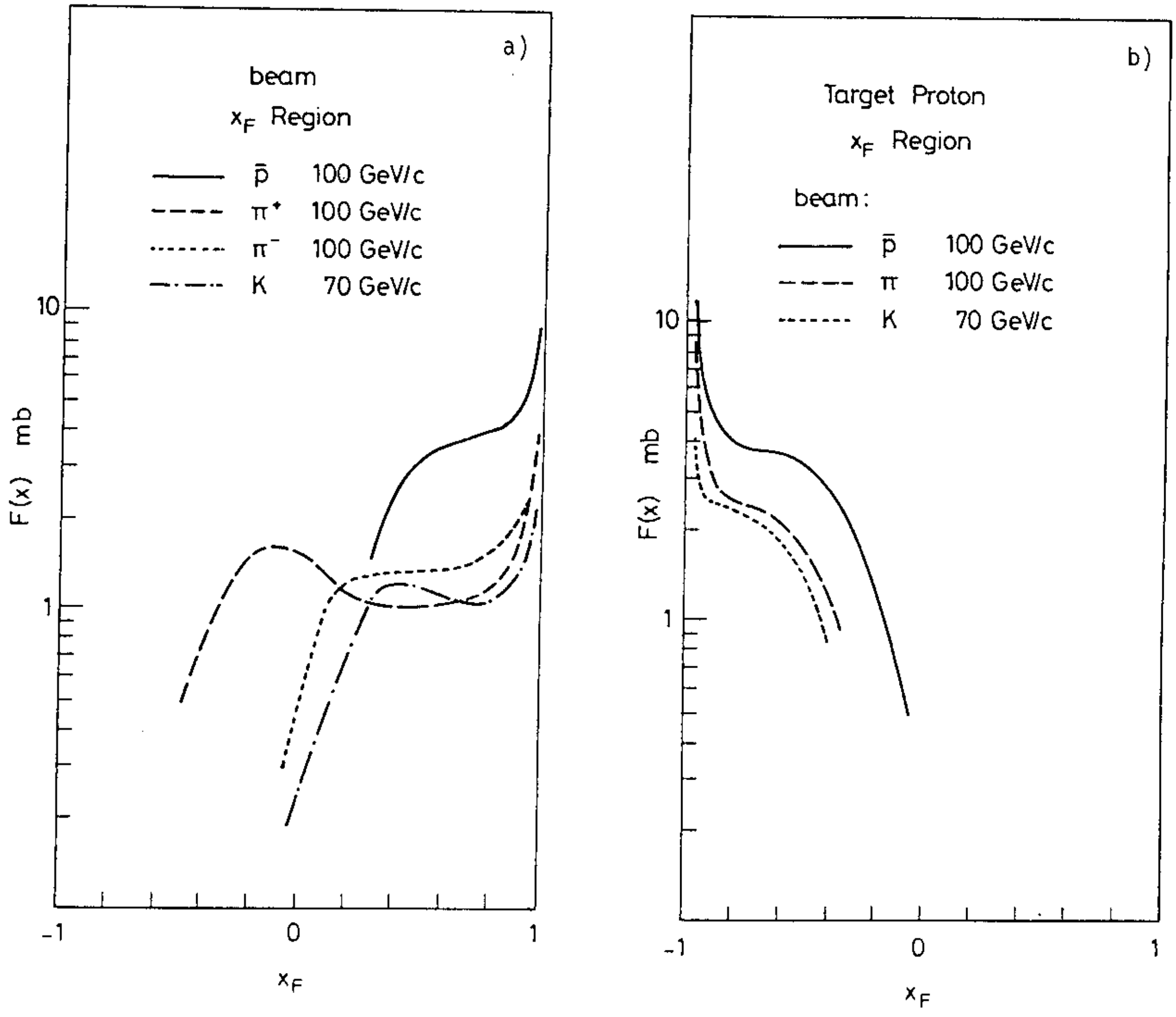
a)
beam
x_F Region
$\bar{p}$ 100 GeV/c
π^+ 100 GeV/c
π^- 100 GeV/c
K 70 GeV/c
10
1
F(x) mb
-1
0
1
x_F
b)
Target Proton
x_F Region
beam:
$\bar{p}$ 100 GeV/c
π 100 GeV/c
K 70 GeV/c
10
1
F(x) mb
-1
0
1
x_F

Fig. 12

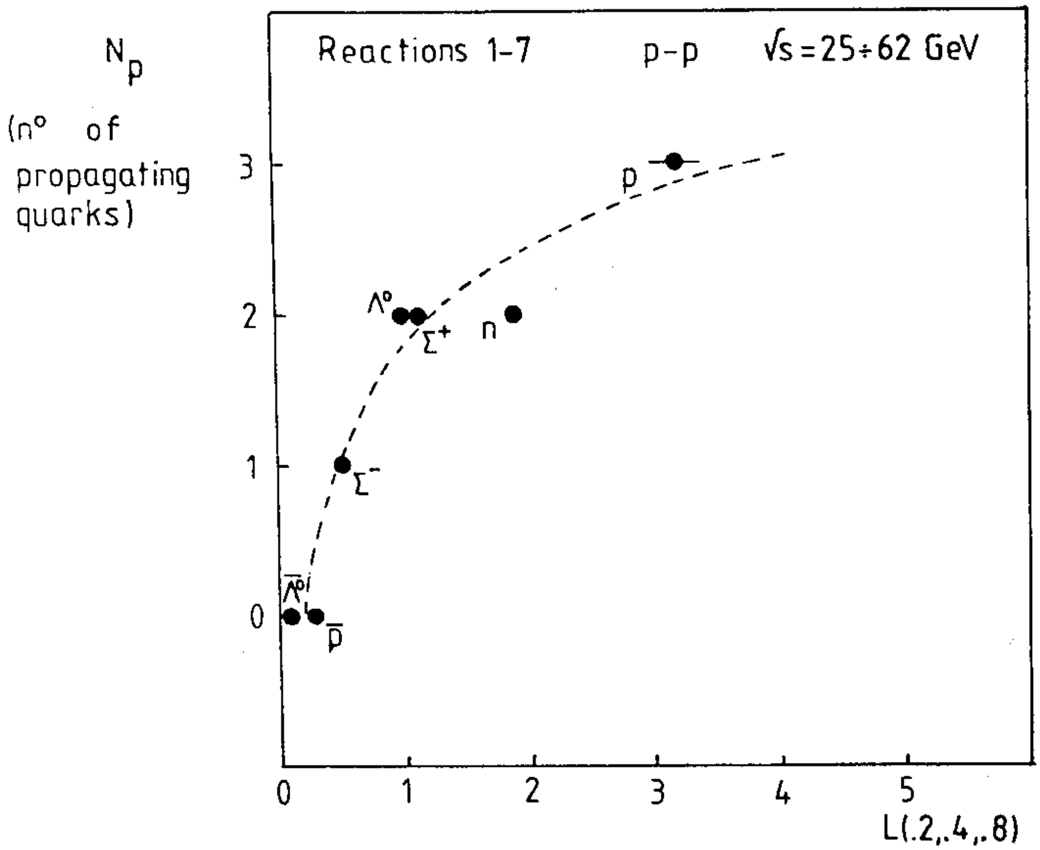
Reactions 1-7
p-p
√s = 25÷62 GeV
N_p
(n° of propagating quarks)
p
Λ^0
Σ^+
n
Σ^-
$\bar{\Lambda}^0$
$\bar{p}$
0
1
2
3
4
5
L(.2,.4,.8)

Fig. 13

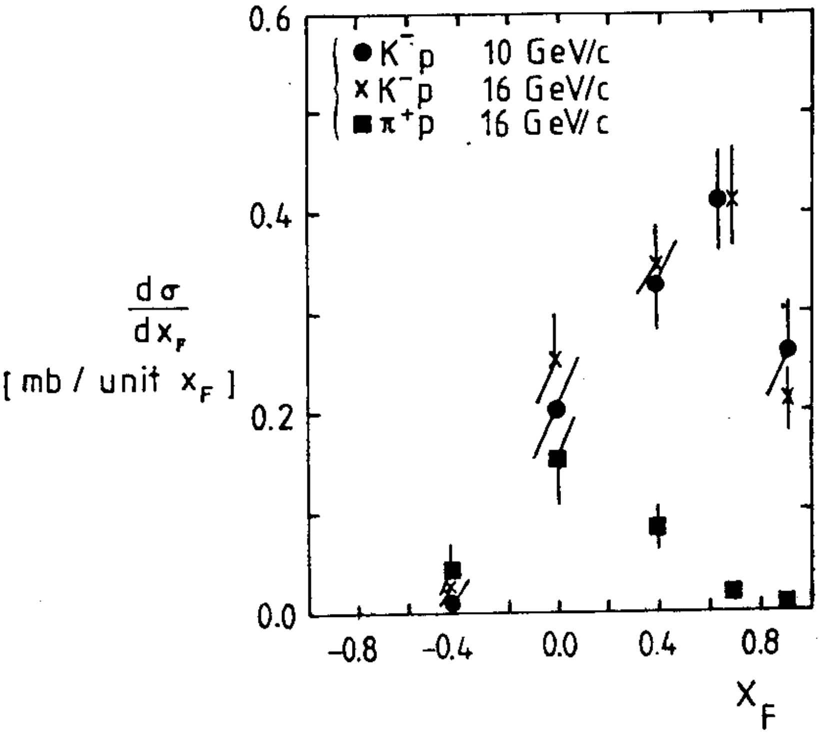
● $K^- p$ 10 GeV/c
× $K^- p$ 16 GeV/c
■ $\pi^+ p$ 16 GeV/c
$\frac{d\sigma}{dx_F}$
[mb / unit x_F]
0.6
0.4
0.2
0.0
-0.8
-0.4
0.0
0.4
0.8
X_F

Fig. 14

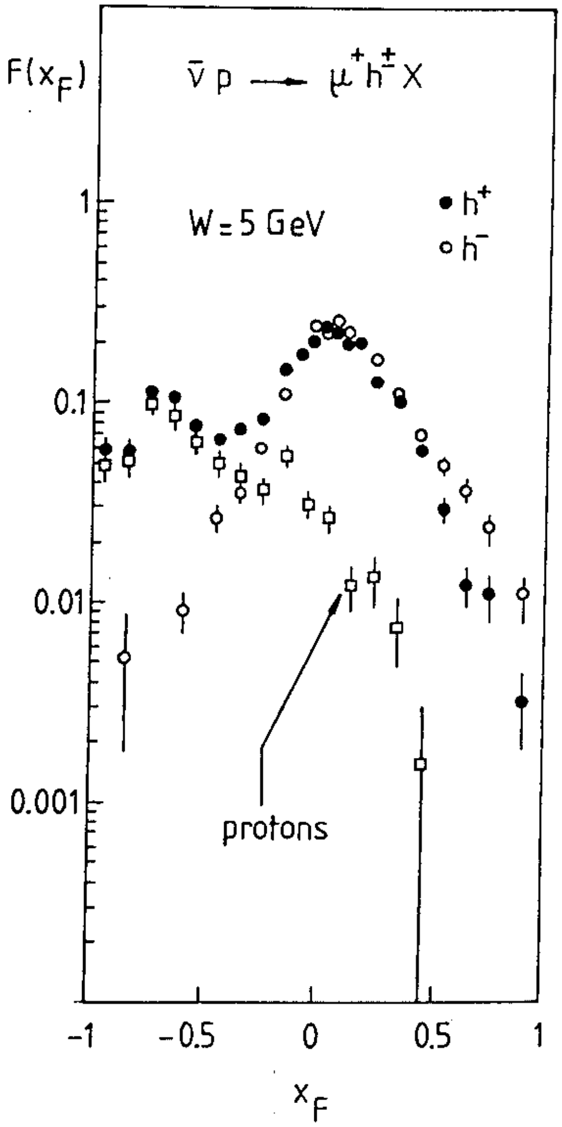

F(x_F)
ν̄ p → μ⁺h± X
W = 5 GeV
● h⁺
○ h⁻
1
0.1
0.01
0.001
protons
-1
-0.5
0
0.5
1
x_F

Fig. 15

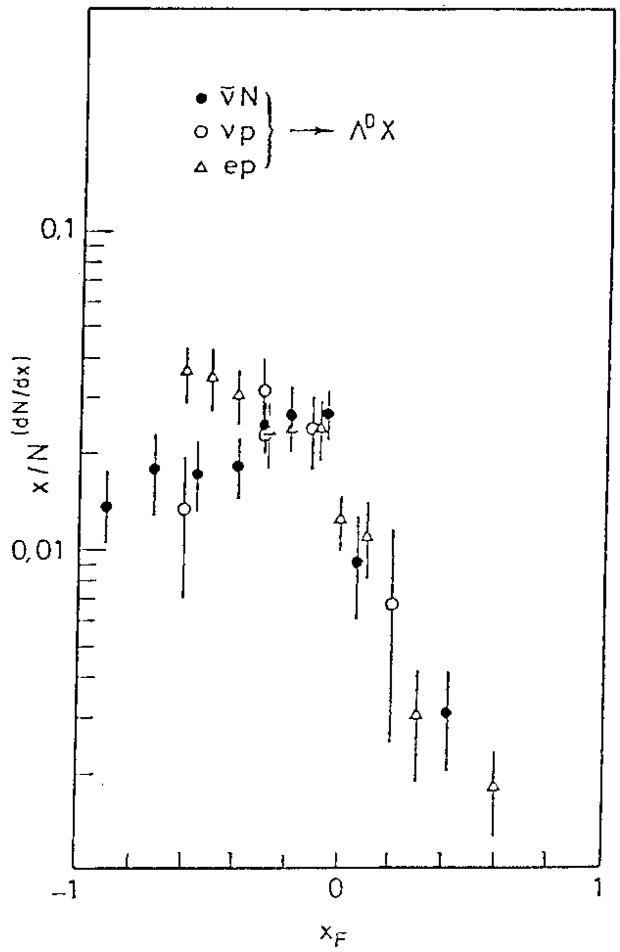

● ν̄N
○ νp
△ ep
→ Λ⁰X
0,1
0,01
x / N (dN/dx)
-1
0
1
x_F

Fig. 16

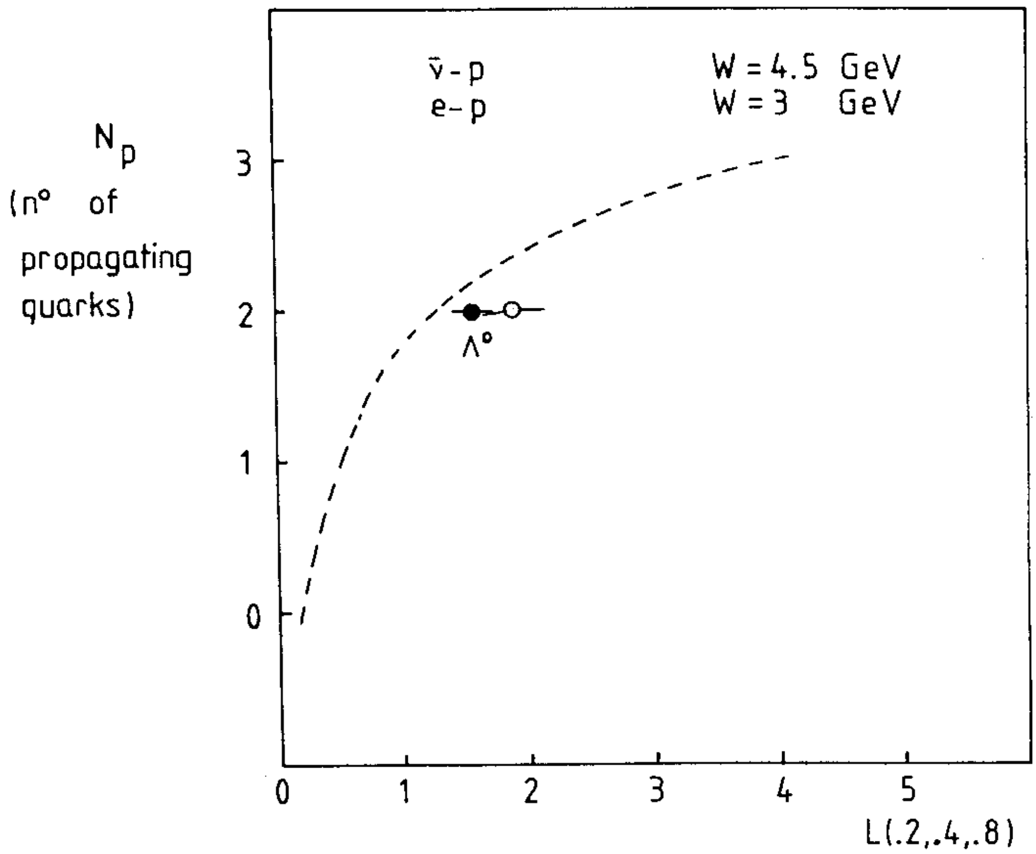

$\bar{\nu}$ - p
e - p
W = 4.5 GeV
W = 3 GeV
N_p
(n° of propagating quarks)
3
2
1
0
Λ^0
0
1
2
3
4
5
L(.2,.4,.8)

Fig. 17